We are thankful to the two reviewers for their thoughtful comments and suggestions. The manuscript was revised accordingly. Listed below are our point-by-point responses in blue to each referee's comments that are repeated in italic.

Response to Reviewer #1

General Comments:

This paper reports real-time aerosol mass spectrometer measurement results at a high altitude level (260m) in Beijing. The aerosol composition, variation, sources, as well as the influence of meteorology were detailedly discussed. As the authors stated, although the ground aerosol measurements were performed a lot before, those at a higher altitude have been rare, and need to be explored to help reveal the formation mechanisms of air pollution in Beijing. Generally, I think this paper provides an interesting dataset and some valuable results for the severe air pollution in China, and could be accepted by ACP after carefully considering the following revisions.

We thank the reviewer's positive comments.

Specific Comments:

The title. Since 260m is still in the range of near ground boundary layer, it is not strict to state that the measurements in this study were "above the urban canopy ".

Urban canopy layer is the layer of air closest to the surface in cities, which is approximately the mean building height (Rotach, 1999). The average building height is approximately 50 m to the south of the sampling site and approximately 20 m for other directions (Song et al., 2013). Considering that the sampling site in this study is located at 260 m, which is well above the urban canopy layer, we used "above the urban canopy" in the title.

Abstract. The description of the vertical differences, which should be the most important feature of this paper, were too vague.

Thank the referee's comments. This paper presented a detailed characterization of aerosol particle composition and sources above the urban canopy in Beijing before and during APEC. In addition to the response of aerosol chemistry to emission controls, the vertical differences are also important and interesting. Following the reviewer's suggestions, we expanded the descriptions of vertical differences in the revised manuscript.

Two different types of aerosol instruments were used simultaneously at two altitudes, including an ACSM and an AMS. Although the two instruments are both based on mass spectrometry, their structures are significantly different. Some comparisons between them ever found that they may have larger difference for high particle concentrations. Were the two instruments systematically compared on the ground before this campaign? This is important to state how much difference between the ground and the 260 m level was from the instruments.

Yes, we did compare the measurements from the two instruments side by side before

the campaign. The HR-AMS and ACSM were deployed for two weeks at the same site with the same inlet. All submicron aerosol species measured by the ACSM were highly correlated with those by the HR-AMS ($r^2 > 0.97$). Although the total NR-PM_1 mass measured by the ACSM agreed well with that by HR-AMS ($r^2 = 0.99$, slope = 0.99), the regression slopes of ACSM against HR-AMS varied from 0.61–1.24 for different aerosol species. Because ACSM was found to have a larger uncertainty in quantification of submicron aerosol species, particularly in determination of relative ionization efficiency, the mass concentrations of aerosol species measured by the ACSM at 260 m were further corrected using the regression slopes of ACSM/HR-AMS obtained from the inter-comparison study. As a result, the comparisons of vertical differences in this study have considered the uncertainties of the two instruments. For clarification, the inter-comparisons between the two instruments were added in the revised manuscript.

Page 22904, Line 17. "Considering that the peak time corresponds to lunch time, we concluded that it was attributed mainly to local cooking sources." This conclusion is too arbitrary. Have the mass spectra at noon been checked for features of cooking emissions?

We thank the referee's comments. As shown in Fig.4, the noon peak of HOA was corresponding well to the lunch time when cooking emissions were significant. To further investigate the influences of cooking sources on organic aerosol (OA) at 260 m, the organic spectra at noon time (10:00-14:00) were extracted and used for PMF analysis. Again, two factors, i.e., HOA and OOA, were identified by PMF analysis. The mass spectra of the two OA factors, which were similar to those from PMF analysis of the entire dataset, are shown in Fig. R1. It is clear that the mass spectrum of Factor1, i.e., HOA, was characterized by a high ratio of *m/z* 55/57 (1.6), which is consistent with the spectral characteristics of fresh cooking aerosols (Mohr et al., 2009;He et al., 2010). In contrast, the traffic-related HOA is generally characterized by comparable *m/z* 55 and *m/z* 57 (Ng et al., 2011). In addition, the diurnal profile of traffic related HOA is often characterized by two peaks at morning and evening rush traffic hours with the lowest concentration occurring at noon time. Therefore, based on the spectral characteristics and diurnal profile of HOA, we concluded that HOA was likely mixed with cooking organic aerosol. It is possible that cooking emissions can be mixed to the height of 260 m due to the high temperature and vertical turbulence exchange in the daytime.

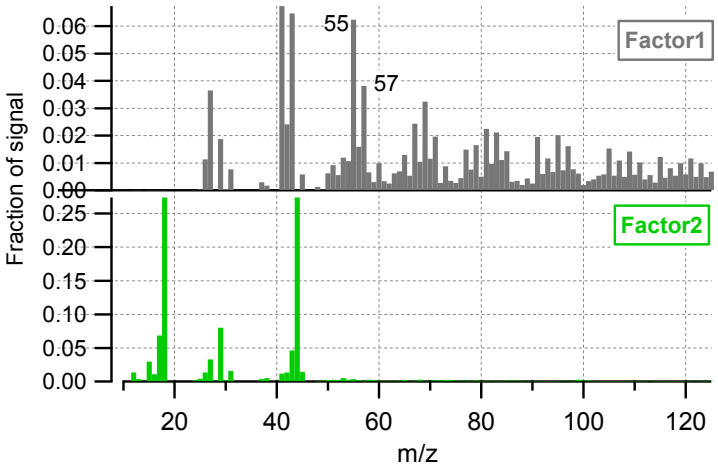

Figure R1. Mass spectra of two factors from PMF analysis of organic aerosol spectra during noon time period (10:00-14:00).

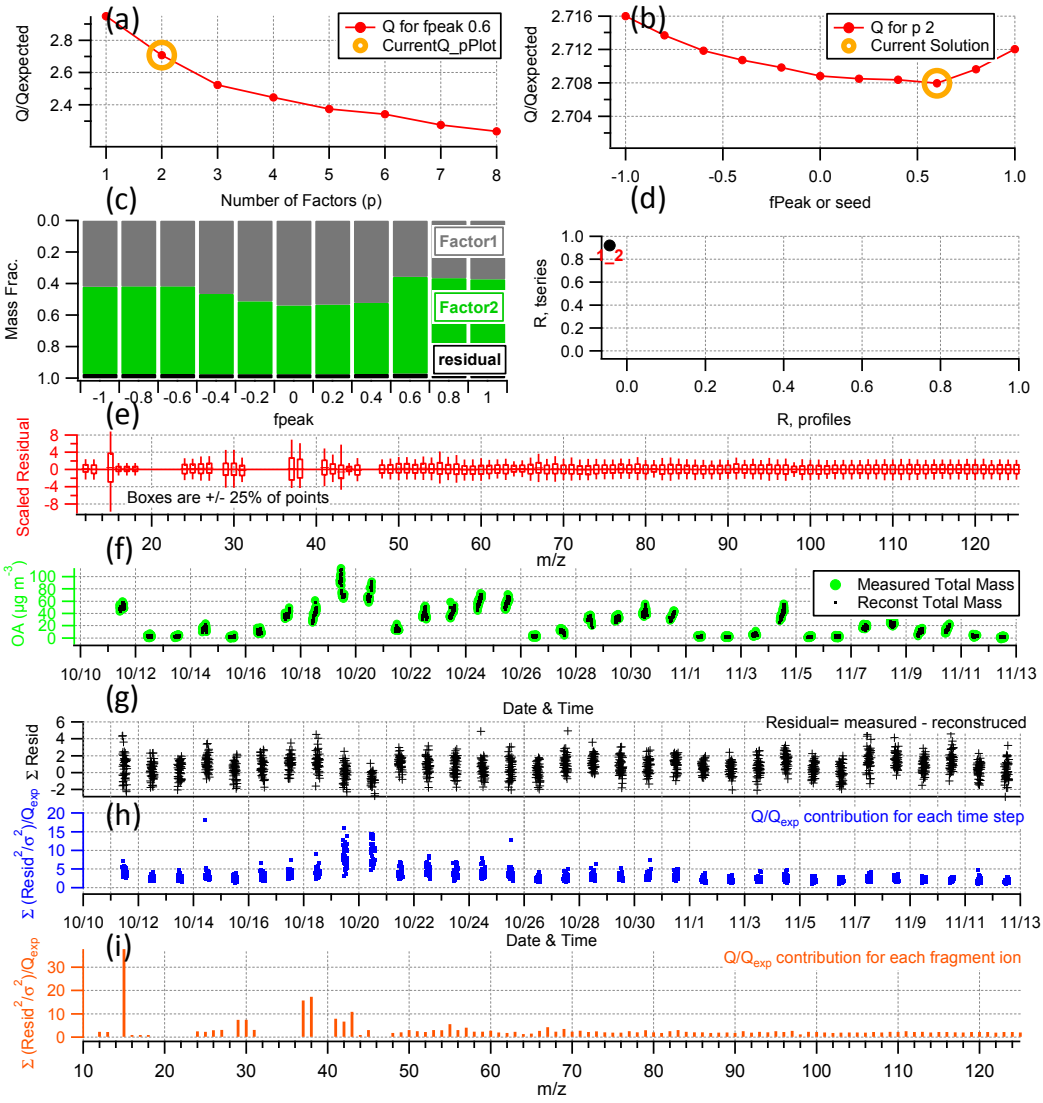

Figure R2. Summary of key diagnostic plots of the noon PMF results for 2-factor solution (fpeak=0.6): (a) Q/Q_{exp} as a function of number of factors (P) selected for PMF modeling. For the 2-factor solution, (b) Q/Q_{exp} as a function of fPeak;(c) fractions of OA factors vs. fPeak, (d) correlations among PMF factors, (e) the box and whiskers plot showing the distributions of scaled residuals for each *m/z*, (f) time series of the measured organic mass and the reconstructed organic mass (two factors), (g) variations of the residual (= measured − reconstructed) of the fit, (h) the Q/Q_{exp} for each point in time, and (i) the Q/Q_{exp} values for each *m/z*.

Fig. 13. This figure may be very misleading if without the comparison between the two instruments, as mentioned above.
Thank the reviewer's comment. The HR-AMS and ACSM were indeed compared before the campaign. The inter-comparisons between the two instruments were now added in Section 2.2 in the revised manuscript (also see our response above).

Page22913, Line 1. A typo of double "cause".
Corrected.

Response to Reviewer #2

General Comments:

This paper presents a case study of pollution and meteorology during the APEC summit in Beijing, with a specific focus on ACSM measurements on the Beijing Meteorological Tower. While the techniques and the processes under investigation are by no means cutting-edge, the facility in unique in its capacity to study pollution and dynamics in a megacity environment. Furthermore, the APEC case study presents a very interesting case that will allow new insights into air quality control strategies and source apportionment to be made. As such, I find this very relevant to ACP. It is worth noting that another paper from this platform and study period, Xu et al., (2015), is also currently under discussion, however having read both papers, I am satisfied that there is not too much overlap because that mainly focuses on the detailed measurements of the HR-AMS. However, while this paper is well-written, I do find that some of the interpretation needs revision and there needs to be more accountability on the PMF and clustering analyses, so therefore I recommend publication subject to the following comments.

We thank the referee's comments.

Specific Comments:

The authors need to include more evidence and reasoning in the supplementary information about their choice of PMF outputs used in the analysis. Specifically, why a 2 factor solution was considered the most reliable and why a nonzero value of fpeak was used.

Thank the referee's comments. PMF analysis of ACSM organic aerosol spectra in this study may not yield higher order factorization as easily due to lower signal-to-noise ratio and the fact that the primary emissions will be homogenized to an extent at the high altitude. As shown in Fig. R3, the time series of the third factor from 3-factor solution is much nosier than the other two factors, and the mass spectrum showed unrealistically high *m/z* 12 and *m/z* 15. Therefore, 2-factor solution was chosen in this study.

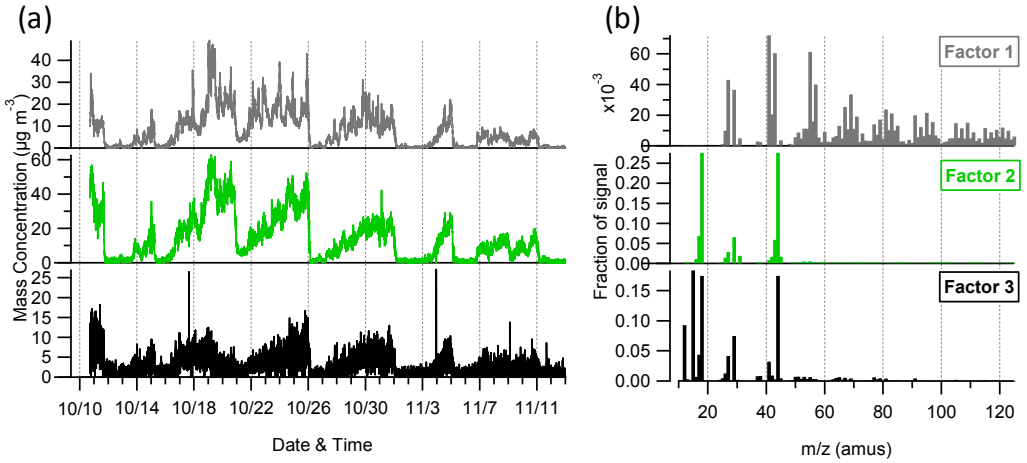

Figure R3. (a) Time series and (b) mass spectra of three OA factors from 3-factor

solution (fpeak=0.4)

We also evaluated the PMF solution as a function of fpeak. While the HOA contribution was fairly stable across different fpeak values (average ±1σ: 39%±4%), the mass spectra were quite different, particularly *m/z* 44. By comparing with the standard spectrum of HOA (Ng et al., 2010) at different fpeaks, we found that the spectrum of HOA at fpeak = 0.4 presented the best correlation (Table S1). The HOA spectrum at fpeak = 0 showed unexpectedly high *m/z* 44 which is a typical characteristics of secondary organic aerosol. Therefore, we chose the solution at fpeak = 0.4 rather than fpeak = 0. Such information was now added in supplementary and also partly in section 2.2 in the revised manuscript.

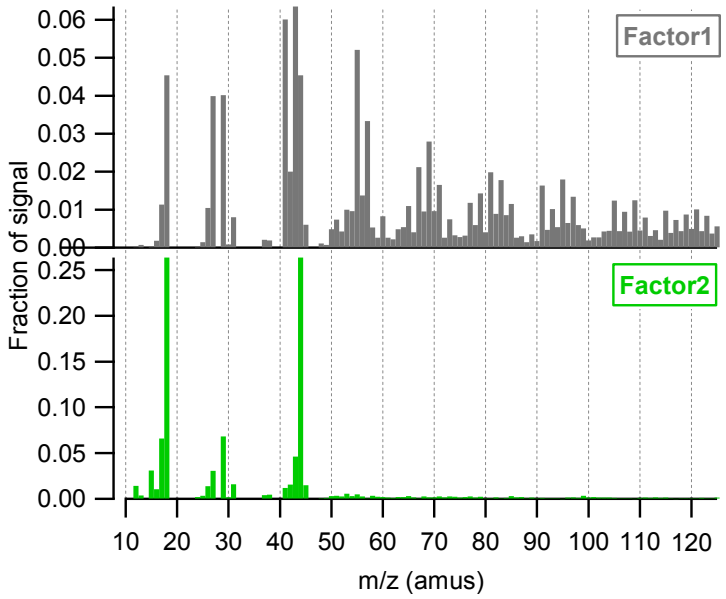

Figure R4. Mass spectra of two OA factors from 2-factor solution at fpeak=0.0

The fact that the authors conclude that the cooking and biomass burning were contained in the HOA factor but could not be resolved begs the question of whether this would be possible using the ME2 algorithm and lead to an improvement in the quality and depth of the science. Have the authors tried doing this?
The individual cooking and biomass burning aerosols were not resolved due to the lower signal-to-noise ratio of the ACSM and also the fact that the primary emissions can be mixed to an extent at a high altitude, e.g., 260 m in this study. The reviewer has a good point that the more advanced analysis with ME-2 algorithm might work for this dataset. Considering this treatment by applying the HR-AMS factor spectra as target profiles for ME-2 analysis would open a whole new avenue of enquiry and introduce new ambiguities to the manuscript, we didn't try ME-2 in this study yet. Nevertheless, we really appreciate the reviewer's suggestions, and will try the ME-2 analysis in the near future.

I do not agree with the conclusions reached regarding aerosol acidity. The correlations on figure 8 are very good and large quantities of nitrate were measured. This to me implies that the aerosol was consistently pH neutral, because an acidic aerosol would not be able to support nitrate in the particle phase. I think it is far more likely that one or more of the inorganic calibration values was wrong. What RIE values did the authors use and how were these determined?

Thank the reviewer's comments. The RIE of ammonium was determined from the pure ammonium nitrate during IE calibration. The default RIEs were used for other species, i.e., 1.4 for organics, 1.1 for nitrate, 1.2 for sulfate, and 1.3 for chloride (Canagaratna et al., 2007). It should be noted that the ACSM concentration was further corrected based on the inter-comparisons with the HR-AMS measurements, particularly for sulfate. By comparing the sulfate concentrations measured by the ACSM and the HR-AMS, a RIE of 0.98 was used for the ACSM sulfate.

We are also surprised the high nitrate content in such acidic aerosols. Similar high concentration of nitrate in acidic aerosols was also observed in previous AMS studies in Beijing (Zhang et al., 2014). Thus, we believe it might be true. There are several reasons which might explain this phenomenon. Firstly, biomass burning aerosol might be an important fraction of HOA in this study as indicated by the prominent *m/z* 60 in the HOA spectrum although it was not resolved. Biomass burning could emit a considerable amount of chloride in the form of KCl rather than NH_4Cl. Therefore, we might overestimate the predicted NH_4^+ when chloride was all counted as NH_4Cl, and hence overestimate the particle acidity. In fact, after excluding chloride, sulfate and nitrate were neutralized for most of the time periods, particularly the low mass loading periods (Fig. R5). These results suggest that chloride in this study might mainly exist in the form of KCl rather than NH_4Cl. In addition, higher acidity was observed at higher mass loading periods as indicated in Fig. R5. This result was consistent with previous findings in Beijing (Zhang et al., 2014). One of the reasons was due to the high humidity during the high mass loading periods. High humidity would facilitate the transformation of acidic gases, e.g., HNO_3 into liquid phase particles. We agree with the reviewer that such high nitrate concentration in acidic environment needs to be interpreted carefully. In the revised manuscript, we expanded the discussions and also the uncertainties on aerosol particle acidity.

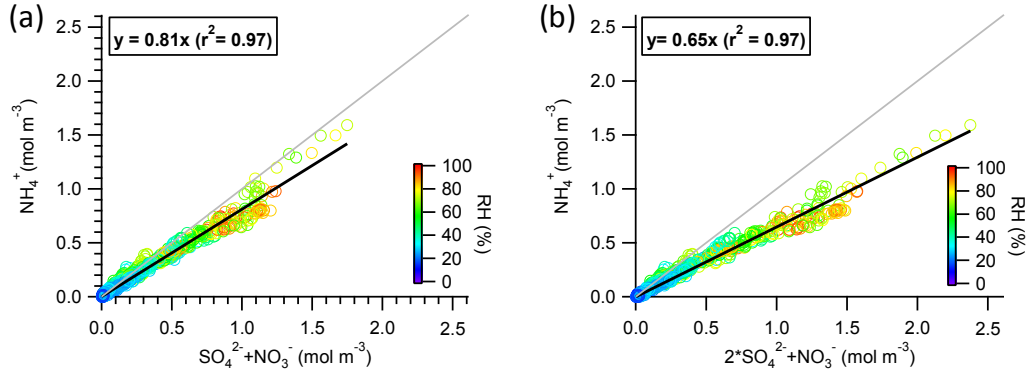

Figure R5. Scatter plots of molar ammonium concentration versus the sum of molar concentrations of sulfate and nitrate (a) $SO_4^{2-}+NO_3^-$, (b) $2*SO_4^{2-}+NO_3^-$. The data were color coded by RH.

The concluding line on page 22906 seems a little out-of-place considering the discussion that follows it concerning back trajectories and sources to the south. Would it not make more sense to talk about the regulatory implications later in the manuscript?

Thank the referee's comments. As suggested, the concluding description was moved to Section 3.2.5.

Insufficient information is given regarding the clustering process applied to the back trajectories. What clustering algorithm was applied? How did the authors determine the optimum number of clusters? The authors should also report the number of trajectories that contribute to each cluster, as well as the percentages, so that their significance can be assessed.

In this study, we calculated the three-day (72 h) back trajectories every hour at 500 m height using Hybrid Single-Particle Lagrangian Integrated Trajectory (HYSPLIT, NOAA) 4.9 model (Draxler and Hess, 1997;Li et al., 2015). The clustering of trajectories is based on the total spatial variance (TSV) method (Draxler et al., 2012). This method minimizes the inter-cluster differences among trajectories while maximizing the inter-cluster differences, which has been widely used in previous studies (Sun et al., 2014;Zhang et al., 2014;Y. J. Li, 2015). Such information was now added in the revised manuscript as "Section 2.3 Air mass trajectory analyses."

Figure R6 shows the change of TSV as function of number of clusters before and during APEC. The changes in TSV decreased substantially from 2 and 3 before and during APEC, respectively. Therefore, the solutions with 3 and 4 clusters before and during APEC were used for further evaluation. We also evaluated 4-cluster solution before APEC. Figure R7 shows the back trajectories results for the 3-cluster solution before APEC. The contribution of cluster1 (C1), cluster 2 (C2), and cluster3 (C3) was 54%, 21%, and 25%, respectively. As shown in Fig. R6a and Fig. 11a, extending the 3-cluster solution to the 4-cluster solution will split C3 into two clusters i.e., C3 and C4. Considering that the APEC period has similar C3 and C4 clusters and also the chemical composition of C3 and C4 in 4-cluster solution were quite different, we chose four clusters before and during APEC for a better comparison of chemical composition and total aerosol loading from the same or similar trajectories before and during APEC.

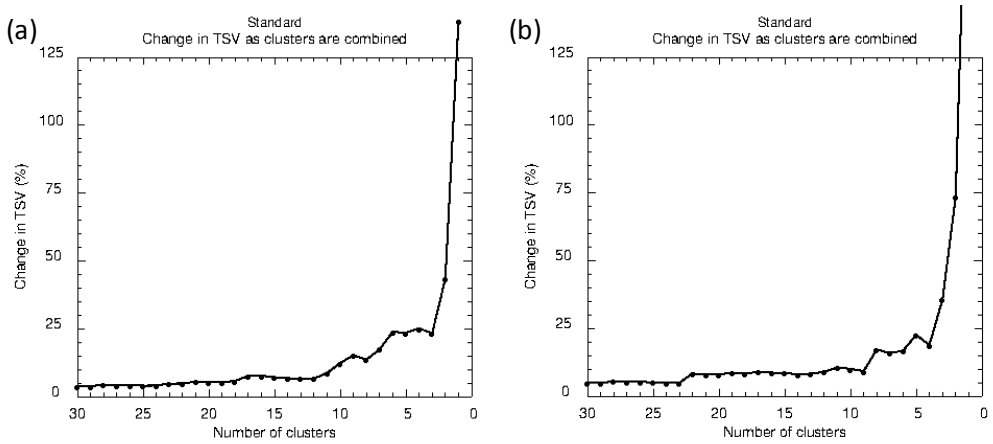

Figure R6. The variation of total spatial variance (TSV) as function of number of clusters **(a)** before and **(b)** during APEC.

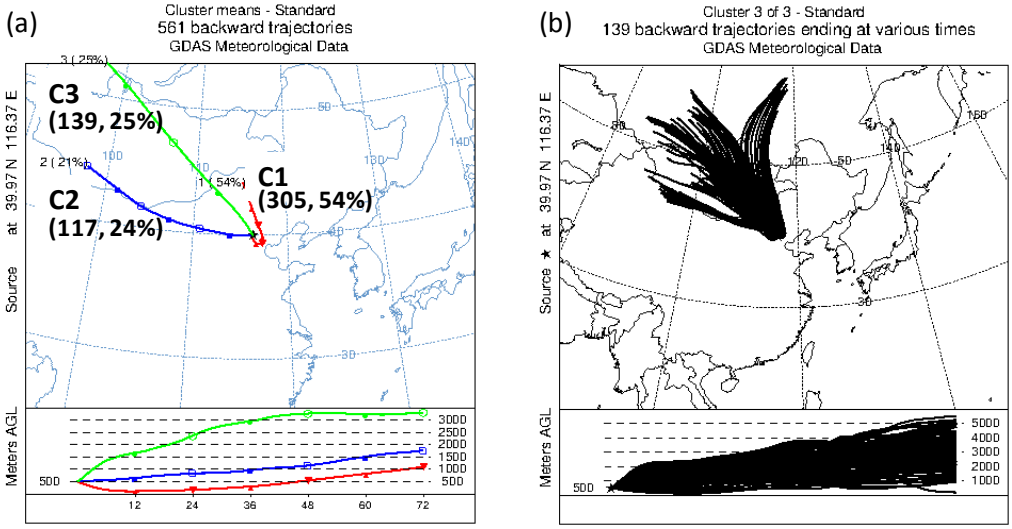

Figure R7. (a) Back trajectory results of 3-cluster solution, and (b) all trajectories of the cluster 3 (C3) before APEC. The number of trajectories and its percentage to the total number of trajectories for each cluster are also shown.

As suggested, the number of trajectories that contribute to each cluster was added on Fig.11 in the revised manuscript.

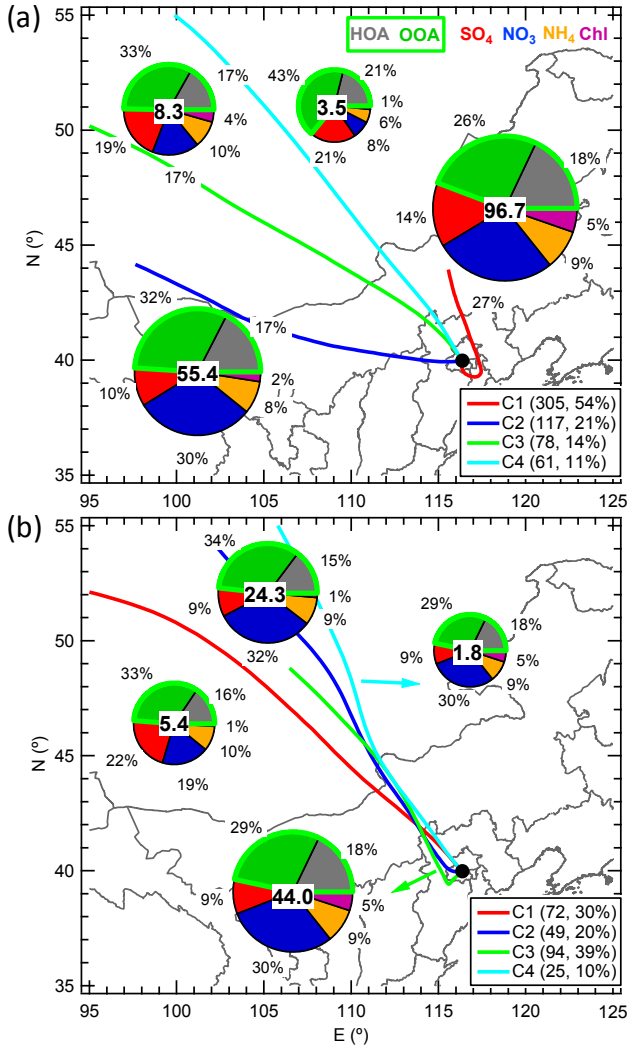

Figure 11. The average NR-PM_1 composition for each cluster **(a)** before and **(b)** during APEC. The numbers on the pie charts refer to the average total NR-PM_1 mass for each cluster. In addition, the number of trajectories and its percentage to the total trajectories are also shown in the legends.

Figures: With the vertical profiles of wind speed and direction, it is not completely clear whether this is from the LIDAR or the in situ measurements. This should be made clearer. Also, the white areas on the plots should be explained.

The vertical profiles of wind speed and wind direction in Fig.1 and Fig. 14 were from the measurements by the Doppler wind lidar. The white areas in the Figure indicate that the data were not available. Other meteorological parameters in the Figures were all from the tower measurements. Following the reviewer's suggestions, we clarified this in the revised manuscript.

References

Canagaratna, M., Jayne, J., Jimenez, J. L., Allan, J. A., Alfarra, R., Zhang, Q., Onasch,

T., Drewnick, F., Coe, H., Middlebrook, A., Delia, A., Williams, L., Trimborn, A., Northway, M., Kolb, C., Davidovits, P., and Worsnop, D.: Chemical and microphysical characterization of aerosols via Aerosol Mass Spectrometry, Mass Spectrom. Rev., 26, 185-222, 2007.

Draxler, R., Stunder, B., Rolph, G., Stein, A., and Taylor, A.: HYSPLIT4 user's guide, version 4, report, NOAA, Silver Spring, Md, in, 2012.

Draxler, R. R., and Hess, G.: Description of the HYSPLIT4 modeling system, Air Resources Laboratory, Silver Spring, Maryland, 1997.

He, L. Y., Lin, Y., Huang, X. F., Guo, S., Xue, L., Su, Q., Hu, M., Luan, S. J., and Zhang, Y. H.: Characterization of high-resolution aerosol mass spectra of primary organic aerosol emissions from Chinese cooking and biomass burning, Atmos. Chem. Phys., 10, 11535-11543, 10.5194/acp-10-11535-2010, 2010.

Li, Y., Lee, B., Su, L., Fung, J., and Chan, C.: Seasonal characteristics of fine particulate matter (PM) based on high-resolution time-of-flight aerosol mass spectrometric (HR-ToF-AMS) measurements at the HKUST Supersite in Hong Kong, Atmos. Chem. Phys., 15, 37-53, 2015.

Mohr, C., Huffman, J. A., Cubison, M. J., Aiken, A. C., Docherty, K. S., Kimmel, J. R., Ulbrich, I. M., Hannigan, M., and Jimenez, J. L.: Characterization of primary organic aerosol emissions from meat cooking, trash burning, and motor vehicles with high-resolution aerosol mass spectrometry and comparison with ambient and chamber observations, Environ. Sci. Technol., 43, 2443-2449, 2009.

Ng, N., Canagaratna, M., Jimenez, J., Zhang, Q., Ulbrich, I., and Worsnop, D.: Real-time methods for estimating organic component mass concentrations from aerosol mass spectrometer data, Environ. Sci. Technol., 45, 910-916, 2010.

Ng, N. L., Canagaratna, M. R., Jimenez, J. L., Zhang, Q., Ulbrich, I. M., and Worsnop, D. R.: Real-Time Methods for Estimating Organic Component Mass Concentrations from Aerosol Mass Spectrometer Data, Environ. Sci. Technol., 45, 910-916, 10.1021/es102951k, 2011.

Rotach, M. W.: On the influence of the urban roughness sublayer on turbulence and dispersion, Atmos. Environ., 33, 4001-4008, http://dx.doi.org/10.1016/S1352-2310(99)00141-7, 1999.

Song, T., Sun, Y., and Wang, Y.: Multilevel measurements of fluxes and turbulence over an urban landscape in Beijing, Tellus B, 65, 2013.

Sun, Y., Jiang, Q., Wang, Z., Fu, P., Li, J., Yang, T., and Yin, Y.: Investigation of the sources and evolution processes of severe haze pollution in Beijing in January 2013, Journal of Geophysical Research: Atmospheres, 119, 4380-4398, 2014.

Y. J. Li, B. P. L., L. Su, J. C. H. Fung, and C.K. Chan: Seasonal characteristics of fine particulate matter (PM) based on high-resolution time-of-flight aerosol mass spectrometric (HR-ToF-AMS) measurements at the HKUST Supersite in Hong Kong, 10.5194/acp-15-37-2015, 2015.

Zhang, J., Sun, Y., Liu, Z., Ji, D., Hu, B., Liu, Q., and Wang, Y.: Characterization of submicron aerosols during a month of serious pollution in Beijing, 2013, Atmos. Chem. Phys., 14, 2887-2903, 2014.

Characteristics and sources of submicron aerosols above the urban canopy (260 m) in Beijing, China during 2014 APEC summit

C. Chen[1,2,3], Y. L. Sun[1,2*], W. Q. Xu[1], W. Du[1,3], L. B. Zhou[1], T. T. Han[1], Q. Q. Wang[1], P. Q. Fu[1], Z. F. Wang[1], Z. Q. Gao[1,2], Q. Zhang[4], D. R. Worsnop[5]

[1]*State Key Laboratory of Atmospheric Boundary Layer Physics and Atmospheric Chemistry, Institute of Atmospheric Physics, Chinese Academy of Sciences, Beijing China*

[2] *Collaborative Innovation Center on Forecast and Evaluation of Meteorological Disasters, Nanjing University of Information Science & Technology, Nanjing, China*

[3]*College of Applied Meteorology, Nanjing University of Information Science and Technology, Nanjing, China*

[3]*Department of Resources and Environment, Air Environmental Modeling and Pollution Controlling Key Laboratory of Sichuan Higher Education Institutes, Chengdu University of Information Technology, Chengdu, China*

[4]*Department of Environmental Toxicology, University of California, 1 Shields Ave., Davis, CA 95616, USA*

[5]*Aerodyne Research, Inc., Billerica, MA, USA*

*Correspondence to Y. L. Sun (sunyele@mail.iap.ac.cn)

Abstract

The megacity of Beijing has experienced frequent severe fine particle pollution during the last decade. Although the sources and formation mechanisms of aerosol particles have been extensively investigated on the basis of ground measurements, real-time characterization of aerosol particle composition and sources above the urban canopy in Beijing is rare. In this study, we conducted real-time measurements of non-refractory submicron aerosol (NR-PM_1) composition at 260 m at the 325 m Beijing Meteorological Tower (BMT) from October 10 to November 12, 2014, by using an aerosol chemical speciation monitor (ACSM) along with synchronous measurements of size-resolved NR-PM_1 composition at near ground level using a High-Resolution Time-of-Flight Aerosol Mass Spectrometer (HR–ToF–AMS). The NR-PM_1 composition above the urban canopy was dominated by organics (46%), followed by nitrate (27%) and sulfate (13%). The high contribution of nitrate and high NO_3^-/SO_4^{2-} mass ratios illustrate an important role of nitrate in particulate matter (PM) pollution during the study period. The organic aerosol (OA) was mainly composed by secondary OA (SOA), accounting for 61% on an average. Different from that measured at the ground site, primary OA (POA) correlated moderately with SOA, likely suggesting a high contribution from regional transport above the urban canopy. The Asia–Pacific Economic Cooperation (APEC) summit with strict emission controls provides a unique opportunity to study the impacts of emission controls on aerosol chemistry. All aerosol species were shown to have significant decreases of 40–80% during APEC from those measured before APEC, suggesting that emission controls over regional scales substantially reduced PM levels. However, the bulk aerosol composition was relatively similar before and during APEC as a result of synergetic controls of aerosol precursors ~~such as SO_2, NO_x, and volatile organic compounds (VOCs)~~. In addition to emission controls, the routine circulations of mountain–valley breezes were also found to play an important role in alleviating PM levels and achieving the "APEC blue" effect. The evolution of vertical differences between 260 m and the ground level was also investigated. Our results show complex vertical differences during the formation and evolution of severe haze episodes that

are closely related to aerosol sources and boundary layer dynamics.

1. Introduction

Beijing (39°56′N, 116°20′ E), the capital of China, is one of the largest megacities in the world with more than 21 million residents and 5.4 million vehicles in operation by the end of 2013 (Beijing Municipal Bureau of Statistics, 2014). In the west, north, and northeast, the city is surrounded by the Taihang and Yanshan mountains at approximately 1000–1500 m above sea level. The fan-shaped topography in addition to the rapid urbanization has caused frequent severe haze pollution episodes in Beijing. These conditions have received a significant amount of attention from atmospheric scientists, the government, and the general public (Sun et al., 2006;Sun et al., 2012a;Sun et al., 2013c;Guo et al., 2014;Sun et al., 2014). For in-depth elucidation of severe urban haze formation and particulate matter (PM) characteristics, extensive studies have been conducted in Beijing including real-time online measurements and filter sampling with subsequent offline analyses (Sun et al., 2006;Pope III et al., 2009;Zhao et al., 2013). Aerosol Mass Spectrometers (AMS), which are capable of determining size-resolved aerosol compositions with high sensitivity, have been widely deployed in Beijing and other cities in China since 2006 (Huang et al., 2012b;Zhang et al., 2014;Li et al., 2015). Numerous conclusions and findings have been obtained since then, which have greatly improved our understanding of aerosol composition, formation mechanisms, and evolution processes (Sun et al., 2010;Xiao et al., 2011;Zhang et al., 2012;Hu et al., 2013;Huang et al., 2013;Guo et al., 2014;Zhang et al., 2014;Li et al., 2015). However, most previous AMS studies include short-term measurements, of generally less than two months, because of the high cost and maintenance of the instrument. The recently developed aerodyne aerosol chemical speciation Monitor (ACSM) (Ng et al., 2011) has been used in some studies for examining the chemical composition, sources, and processes of atmospheric aerosols in China. The advantage of the ACSM is its robustness for real-time long-term measurements of aerosol particle composition with little attendance (Ng et al., 2011;Sun et al., 2012a;Sun et al., 2013c;Budisulistiorini et al., 2014;Sun et al.,

2014;Parworth et al., 2015;Petit et al., 2015). The first ACSM measurements in Beijing highlighted the important role of nitrate in PM pollution in summer, which was mainly attributed to the partitioning of nitric acid into liquid ammonium nitrate particles (Sun et al., 2012a). The PM pollution characteristics also dramatically differed between summer and winter. Agricultural burning and photochemical production play major roles in PM pollution in summer (Li et al., 2010;Huang et al., 2012a;Sun et al., 2012a;Zhang et al., 2015), whereas coal combustion is the dominant source of PM in winter (Sun et al., 2013c). A more detailed analysis of a severe haze pollution episode occurred in January 2013 suggested that stagnant meteorological conditions, source emissions, secondary production and regional transport are four major factors driving the formation and evolution of haze pollution in Beijing during winter (Sun et al., 2013c;Guo et al., 2014;Sun et al., 2014;Zhang et al., 2014).

Despite extensive efforts for the characterization of fine particle pollution in Beijing, most studies are conducted at ground sites, which are subject to significant influences of local emission sources such as traffic, cooking, and biomass burning. In comparison, measurements obtained above the urban canopy with much less influence of local source are more representative for a large scale, which is of great importance for characterizing regional transport. However, such studies in Beijing are rare due to the absence of high platforms. The 325 m Beijing Meteorological Tower (BMT) is a unique platform for measuring aerosol and gaseous species at various heights in Beijing megacity. Moreover, this platform is beneficial for studying the interactions of the lower boundary layer (<300 m) and air pollution, particularly during autumn and winter when the nocturnal planetary boundary height is often below 300 m (Ting et al., 2008;Zhang et al., 2013). Based on the BMT measurements, Sun et al.~~(Sun et al., 2009;Sun et al., 2013a)~~ (2009;2013a) reported that the SO_2 concentration reached its maximal value at 50 m during heating periods, whereas $PM_{2.5}$ showed a "higher top and lower bottom" vertical pattern due to the inversions of temperature (*T*) and relative humidity (RH) during summer hazy days. Guinot et al. (2006) and Meng et al. (2008) also determined that local concentration peaks at 50 m to 100 m were likely related to the urban canopy. However, real-time characterization of aerosol particle

composition above the urban canopy has been performed only once (Sun et al., 2015). The two-week study found substantially different aerosol compositions between ground level and 260 m. In addition, the compositional differences at the two heights were found to be strongly associated with source emissions, the vertical mixing mechanism, and RH/*T*-dependent secondary production. Because these measurements only lasted two weeks, the aerosol characteristics and sources above the urban canopy remain poorly understood.

The 2014 Asia–Pacific Economic Cooperation (APEC) summit was hosted in Beijing during November 5–11, 2014, when strict emission control measures were implemented in Beijing and surrounding regions to ensure the air quality. During November 3–12, emission controls such as reducing the number of vehicles in operation by approximately 50%, shutting down factories, stopping construction activities, and enhancing the cleanliness of urban roads were gradually implemented (http://www.bjepb.gov.cn/bjepb/323474/331443/331937/333896/412827/index.html, in Chinese). The neighboring provinces such as Hebei, Tianjin, and Shandong implemented the same emission controls during APEC (http://www.bjepb.gov.cn/bjepb/324122/412670/index.html, in Chinese). As a result, the PM levels in Beijing during the summit were significantly reduced, leading to "APEC blue," a phrase commonly used to refer to the good air quality. However, the response of aerosol chemistry to emission controls over a regional scale has not been investigated. Measurements above the urban canopy are ideal for evaluating the roles of emission controls in reducing PM levels under the condition of minimizing the influences of local point sources.

In this study, we conduct real-time measurements of non-refractory submicron aerosol (NR-PM_1) composition including organics (Org), sulfate (SO_4^{2-}), nitrate (NO_3^-), ammonium (NH_4^+), and chloride (Cl^-) at 260 m at the BMT before and during APEC, October 10–November 2 and November 3–12, 2014, respectively, by using an ACSM. The aerosol composition, diurnal variation, and sources above the urban canopy are investigated in detail. The responses of aerosol composition, particle acidity, and sources of organic aerosol (OA) to emission controls are elucidated by

142 comparing the changes before and during APEC, and the roles of meteorological
143 conditions in PM reduction during APEC are discussed. In addition, the vertical
144 differences of aerosol composition and its interactions with boundary layer dynamics
145 are also examined.
146
147 **2. Experimental Methods**
148 **2.1 Sampling site and measurements**
149 All of the measurements in this study were conducted at the same site as that
150 reported by Sun et al. (2013c), which is an urban site at the Institute of Atmospheric
151 Physics, Chinese Academy of Sciences, between North 3rd and 4th Ring Road from
152 October 10 to 12 November, 2014. The ACSM and gas measurement instruments
153 were mounted inside a container at 260 m on the BMT. The ACSM sampling setup
154 used in this study is similar to that described by Sun et al. (2012a). Briefly, aerosol
155 particles were first sampled into the container with a $PM_{2.5}$ cyclone to remove coarse
156 particles larger than 2.5 μm. After passing through a diffusion silica-gel dryer, aerosol
157 particles were sampled into the ACSM at a flow rate of ~0.1 L/min. The ACSM was
158 operated by alternating ambient air and filtered air with a mass spectrometer at a
159 scanning rate of 500 ms amu^{-1} from *m/z* 10 to 150. The data were saved every two
160 cycles, leading to a time resolution of approximately 5 min. The detailed principles of
161 the ACSM can be found elsewhere (Ng et al., 2011;Sun et al., 2012a). An Aerodyne
162 High-Resolution Time-of-Flight AMS (HR-ToF-AMS) was simultaneously deployed
163 near the ground level at the same location to measure the size-resolved NR-PM_1
164 aerosol composition. Details of the sampling and operation procedures of the
165 HR-ToF-AMS was given in Xu et al. (2015).
166 Meteorological variables including wind speed (WS), wind direction (WD), RH,
167 and *T* at 15 heights of 8, 15, 32, 47, 65, 100, 120, 140, 160, 180, 200, 280, and 320 m
168 were obtained from the BMT. In addition, a Doppler wind lidar (Windcube 200,
169 Leosphere, Orsay, France) was deployed at the same location to obtain the wind
170 profiles from 100 m to 5000 m with a spatial resolution of 50 m and a time resolution
171 of 10 min. All of the data in this study are reported in Beijing Standard Time (BST),

which ~~is equivalent to~~ equals ~~to~~ Coordinated Universal Time (UTC) plus 8 h.

2.2 Data Analysis

The ACSM data were analyzed for the mass concentration and chemical composition of NR-PM_1 species including organics, sulfate, nitrate, ammonium, and chloride by using ACSM standard data analysis software (v. 1.5.3.0). Detailed analytical procedures have been reported by Ng et.al (2011) and Sun et.al (2012a). Similar to that in previous studies in Beijing (Sun et al., 2011;Sun et al., 2012a;Sun et al., 2013c;Sun et al., 2014), an empirical and constant collection efficiency (CE) of 0.5 was applied during the entire campaign to compensate for the particle loss due mainly to particle bounce at the vaporizer (Matthew et al., 2008). The CE of 0.5 is rationale for this study because aerosol particles were dried, and the mass fraction of ammonium nitrate was overall below the threshold value (40%) that affects CE (Middlebrook et al., 2012). The average ratio of measured NH_4^+ ($NH_4^+{}_{meas}$) versus predicted NH_4^+ ($NH_4^+{}_{pred}$) was 0.56, suggesting that the aerosol particles were acidic. Although the particle acidity would have a slightly higher CE than 0.5 (~0.59) if the equation $CE_{dry} = \max(0.45, 1.0 - 0.73 \times (NH_4^+{}_{meas}/NH_4^+{}_{pred}))$ recommended by Middlebrook et al. (2012) were used, no effect on CE is present if using the parameterization reported by Quinn et al. (2006). For consistency with our previous studies and with the HR-ToF-AMS measurements at the ground site, we maintained CE = 0.5 in this study. The default relative ionization efficiency (RIE) values, 1.4 for organics, 1.1 for nitrate, 1.2 for sulfate, and 1.3 for chloride except ammonium (6.5) which was determined from pure ammonium nitrate particles. Note that the ACSM measurements were compared with those of HR-AMS at the same location before the campaign. All submicron aerosol species measured by the ACSM were highly correlated with those by the HR-AMS ($r^2 > 0.97$). Although the total NR-PM_1 mass measured by the ACSM agreed well with that by HR-AMS ($r^2 = 0.99$, slope = 0.99), the regression slopes of ACSM against HR-AMS varied from 0.61–1.24 for different aerosol species. Because ACSM was found to have a larger uncertainty in quantification of submicron aerosol species, particularly in determination of relative ionization efficiency, the mass concentrations of aerosol species measured by the

ACSM at 260 m were further corrected using the regression slopes of ACSM/HR-AMS obtained from the inter-comparison study.

Positive matrix factorization (PMF) with the PMF2.exe algorithm (Paatero and Tapper, 1994) was performed on the ACSM OA mass spectra to resolve potential OA components with different sources and processes. Only *m/z*'s < 125 was included in the PMF analysis due to the large interferences of naphthalene signals on several larger *m/z*'s (e.g., *m/z* 127–129) (Sun et al., 2012a;Sun et al., 2013c;Sun et al., 2014). The PMF results were then evaluated by using an Igor Pro-based PMF Evaluation Tool (PET, v 2.06) (Ulbrich et al., 2009) with following procedures detailed by Zhang et al. (2011). After careful evaluation of the mass spectra and time series of OA factors, a two-factor solution, i.e., an oxygenated OA (OOA) and a hydrocarbon-like OA (HOA) with fpeak = 0.4, was chosen. A more detailed PMF diagnostics is presented in Figs. S1, S2 and Table S1. While the 3-factor solution resolved an unrealistic factor with unexpectedly high *m/z* 12 and *m/z* 15, the 2-factor solution at fpeak = 0 showed much higher *m/z* 44 in HOA spectrum, which is generally a characteristics of OOA (Fig. S3).

2.3 Air mass trajectory analyses

The three-day (72 h) back trajectories were calculated every hour at 500 m height using the Hybrid Single-Particle Lagrangian Integrated Trajectory (HYSPLIT, NOAA) 4.9 model (Draxler and Hess, 1997;Li et al., 2015). The trajectories were then grouped into four clusters before and during APEC using the algorithm of cluster analysis. The clustering of trajectories is based on the total spatial variance (TSV) method (Draxler et al., 2012). This method minimizes the inter-cluster differences among trajectories while maximizing the inter-cluster differences, which has been widely used in previous studies (Sun et al., 2014;Zhang et al., 2014;Li et al., 2015)

Formatted: Not Highlight
Formatted: Indent: First line: 0.29"
Formatted: Not Highlight
Formatted: Not Highlight
Formatted: Not Highlight
Formatted: Not Highlight
Formatted: Not Highlight

3. Results and discussion

3.1 General description

3.1.1 Submicron aerosol and meteorology

The NR-PM_1 mass concentration varied significantly from 0.7 to 254 μg m^{-3}, with an average of 53.5 μg m^{-3}. As indicated in Fig. 1, the variations of NR-PM_1 were

strongly associated with WD and WS. The formation of severe haze episodes was generally initiated by a WD change from northerly to southerly and a decrease of WS to less than 5 m s^{-1} below 1 km. The southern air flow and low WS were then dominant most of the time during the evolution of haze episode; subsequently, the air masses changed from the south to the north/northwest, leading to a rapid decrease of PM level in a few hours. Haze episodes with such life cycle driven by meteorological conditions have also been observed many times in Beijing (Jia et al., 2008;Sun et al., 2013c;Guo et al., 2014;Sun et al., 2014). Note that a mountain–valley breeze lasting approximately half a day was frequently observed throughout the study, which reduced the daytime PM levels to a certain degree. As shown in Fig. 1, most of the cleaning processes were similar, all driven by the switch of air masses from south/southwest to north/northwest associated with high WS across the entire vertical layer (>5 m s^{-1}). However, the cleaning process occurring on October 20–21 was different. As the WD changed from the south to the northwest/northeast, the NR-PM_1 concentration remained high. This phenomenon can be explained by the low WS (<4 m s^{-1}) below 500 m and the high RH (Figs. 2, S4~~2~~). The NR-PM_1 began to decrease at ~20:00 as WD shifted to the south associated with a decrease in RH. This result indicates that a cleaner and dryer air mass was located to the south of Beijing during this stage. Such a cleaning process by southern air flow is not common and is generally weaker than that by northern/northwestern flow. This observation is supported by the higher NR-PM_1 concentration of ~20 μg m^{-3} on October 21 than during other cleaning periods at ~<5 μg m^{-3}. The average mass concentration of NR-PM_1 during APEC was 24.1 μg m^{-3}, which is significantly lower than the 65.1 μg m^{-3} recorded before APEC, indicating a large reduction of PM during APEC. In addition, the southern air mass occurred less frequently and had a shorter duration during APEC. These results manifest that meteorology in addition to emission controls might have played an important role in reducing PM levels during APEC.

The NR-PM_1 species showed similar and dramatic variations to the total NR-PM_1 mass (Fig. 2). In particular, three haze episodes before APEC (Ep1, Ep2, and Ep3 in Fig. 2d) and two episodes during the summit (APEC1 and APEC2 in Fig. 2d) were

observed in this study. The three episodes before APEC were all characterized by high RH at 48–70% and low WS at 2.3–3.4 m s^{-1}, elucidating the important roles of stagnant meteorological conditions in severe haze formation. In comparison, the RH in the two episodes during APEC was lower at 34–38%, and the WS was comparably higher at 3.1–3.8 m s^{-1} (Table 1). These results suggest that the meteorological conditions during APEC appeared to be more favorable for dispersion of pollutants. Indeed, clear accumulation processes of aerosol species were observed for three episodes before APEC, yet they were much weaker during the summit. However, the two episodes during APEC showed obvious temperature inversions, which inhibited the vertical convection of pollutants. The meteorological conditions during haze episodes differed substantially from those during clean periods, which were characterized by high WS at >5 m s^{-1} and low RH at <20%.

The NR-PM_1 was dominated by organics, accounting for on average 46% of the total mass, followed by nitrate at 27%, sulfate at 13%, ammonium at 9%, and chloride at 5%. The nitrate contribution ranged from 27% to 28% during the three episodes before APEC and from 29% to 31% in the two episodes during APEC, which is significantly higher than the sulfate contribution of 10–15% and 8–11%, respectively (Fig. 6). Although the dominance of organics in PM_1 was consistent with that in previous studies in Beijing (Sun et al., 2012a;Sun et al., 2013c;Guo et al., 2014;Sun et al., 2014;Zhang et al., 2014), the nitrate contribution in this study was approximately twice that of sulfate and significantly higher than previously reported values of 16% in 2011 (Sun et al., 2013c) and 13–14% in 2013 (Sun et al., 2014;Zhang et al., 2014). The mass ratio of NO_3^-/SO_4^{2-} can be used to indicate the relative importance of mobile and stationary sources (Arimoto et al., 1996). Therefore, higher NO_3^-/SO_4^{2-} in this study likely indicates the predominance of mobile source rather than stationary source. Because the continuous increase of NO_x emissions associated with a decrease in SO_2 (Wang et al., 2013), nitrate is expected to play a more important role in PM pollution in the future. Our results highlight that NO_x emission control should be a priority in mitigating air pollution, particularly in non-heating seasons with low SO_2 precursors.

Figure 3 further shows the time series of NO_3^-/SO_4^{2-} mass ratio and sulfur oxidation ratio (SOR) calculated as the molar fraction of sulfate in total sulfur (i.e., sulfate and SO_2) (Sun et al., 2014). The NO_3^-/SO_4^{2-} was ubiquitously greater than 1 during five haze episodes, indicating the importance of nitrate in the formation of severe haze pollution. Interestingly, we observed a rapid increase in NO_3^-/SO_4^{2-} during the formation stage of a pollution episode followed by a decrease in NO_3^-/SO_4^{2-} during the subsequent evolution stage. The variations of NO_3^-/SO_4^{2-} illustrate that two different formation mechanisms might drive the formation and evolution of haze episodes. During the early stage of haze formation, the RH was relatively low and the formation rate of sulfate was correspondingly low, which is supported by the low SOR values. Consequently, the nitrate formation played a dominant role during this stage. The SO_4^{2-} concentration remained consistently low when the nitrate began to increase (Fig. 2d). As the RH continued to increase, the SOR showed a corresponding increase indicating that more SO_2 was oxidized to form sulfate, most likely via aqueous-phase processing (Zhang and Tie, 2011;Sun et al., 2013b). The SO_4^{2-} concentration then showed a substantial increase, and the NO_3^-/SO_4^{2-} ratio decreased as a result. For example, during Ep2, the hourly NO_3^-/SO_4^{2-} increased from ~1.1 to 4.0 during the formation stage and then decreased to ~1.8 during the evolution stage. These results indicate that SO_4^{2-} played an enhanced role in PM pollution during the evolution stage of haze episodes with high RH. Moreover, the NO_3^-/SO_4^{2-} ratios during clean periods (~0.3) were much lower than those during haze episodes. One explanation is that the nitrate in clean air masses from north/northwest is significantly lower than that of sulfate.

3.1.2 Sources and composition of OA

Two OA factors, HOA and OOA, were identified in this study. The HOA spectrum was similar to those determined at other urban sites (Huang et al., 2012a;Sun et al., 2012a;Sun et al., 2012b), which is characterized by prominent hydrocarbon ion peaks of *m/z* 27, 29, 41, 43, 55, 57 (Fig. 4a). The HOA spectrum showed a higher *m/z* 55/57 ratio compared with that of exhaust aerosols from diesel trucks and gasoline vehicles (Mohr et al., 2009), yet it had characteristics similar to

those resolved in urban Beijing (Sun et al., 2010;Sun et al., 2012a). The high *m/z* 55/57 ratio and the two visible peaks at meal times in diurnal variations (Fig. 4b) indicate the impact of local cooking activities (Sun et al., 2011;Sun et al., 2012a;Sun et al., 2013c). However, the two HOA peaks were much smaller than those observed at the ground site (Xu et al., in preparation), indicating a significantly smaller impact of local cooking emissions on OA at 260 m. Moreover, the HOA spectrum showed a considerable *m/z* 60 peak, a marker *m/z* for biomass burning (Aiken et al., 2009;Huang et al., 2011;Zhang et al., 2015). The fraction of *m/z* 60 was 0.9%, which is much higher than ~0. 3% in the absence of biomass burning. All these results suggest that HOA was a primary OA factor combined with traffic, cooking, and biomass burning emissions. Limited by the ACSM spectra and PMF analysis, we were not able to separate the different primary OA factors in this study. HOA correlated well with chloride ($r^2 = 0.61$) and moderately well with secondary inorganic species ($r^2 = 0.42–0.65$), indicating that a major fraction of HOA shared similar sources to secondary species at 260 m, which was likely from regional transport. HOA on average contributed 39% of total organics, which is less than the 57% observed at the ground site during the same study period (Xu et al., in preparation). This result indicates a smaller impact of primary sources above the urban canopy. The diurnal cycle of HOA was relatively flat with two visible peaks occurring at noon and night. The HOA contribution to OA was relatively constant throughout the day, ranging from 36% to 43%. This result further supports the theory that HOA above the urban canopy was dominantly from regional transport and was well mixed with regional secondary OA (SOA). Indeed, the correlation of HOA with OOA in this study was quite high ($r^2 = 0.76$), supporting that HOA and OOA might have some common sources (e.g., regional transport) at 260 m.

The mass spectrum of OOA resembles that identified in 2012 in summer in Beijing (Sun et al., 2012a) in addition to those resolved at other urban sites (Ulbrich et al., 2009), which is characterized by a prominent *m/z* 44 peak (mainly CO_2^+). OOA dominated the OA composition throughout the day, ranging from 57% to 64%. The average OOA contribution to OA was 61%, which is close to those previously

reported in Beijing (Huang et al., 2010;Sun et al., 2012a;Sun et al., 2013c). The diurnal cycle of OOA was relatively flat, yet a gradual increase during the day was also observed despite the rising planetary boundary layer, suggesting daytime photochemical processing. OOA is often considered as a good surrogate of SOA (Zhang et al., 2005;Jimenez et al., 2009;Ng et al., 2011). In this study, OOA tracked well with secondary inorganic species such as NO_3^-, SO_4^{2-} (r^2 = 0.72–0.90), which is consistent with previous conclusions that OOA is a secondary species in nature (Zhang et al., 2005;Sun et al., 2012a).

3.2 Response of aerosol chemistry to emission controls

3.2.1 Aerosol composition

Figure 5 shows the variations of aerosol composition as a function of NR-PM_1 mass loading before and during APEC. The organics contribution showed a notable decrease from 62% to 32% as the NR-PM_1 mass concentration increased from <10 μg m^{-3} to >200 μg m^{-3} before APEC. In contrast, the sulfate contribution showed a corresponding increase from 8% to 22%. Except for low values at NR-PM_1 <10 μg m^{-3}, nitrate and ammonium constituted relatively constant fractions of NR-PM_1 across different NR-PM_1 loadings and varied at 21–31% and 8–12%, respectively. These results highlighted the enhanced roles of secondary inorganic species in severe PM pollution before APEC. This observation is further supported by a comparison of average chemical composition between three pollution episodes and a clean event (Fig. 6). The secondary inorganic aerosol (SIA = SO_4^{2-} + NO_3^- + NH_4^+) on average contributed 46–51% of the total NR-PM_1 mass during the three episodes before APEC, which is significantly higher than the 40% reported during the clean event (Fig. 6). The NR-PM_1 mass loading-dependent aerosol composition showed a different behavior during APEC. As shown in Fig. 5b, all aerosol species had relatively constant contributions to NR-PM_1 at 10–100 μg m^{-3}. The contribution of organics ranged from 43% to 58%, which is overall higher than those before APEC. This result indicates an enhanced role of organics during APEC, particularly during severe PM pollution periods. Similarly, nitrate contributed the largest fraction of NR-PM_1, varying from 23% to 32%. Figure 5 also shows a very broad range of NR-PM_1 mass

concentration with the maximum concentration over 200 μg m^{-3} before APEC. In contrast, the range of NR-PM_1 was much narrower during APEC, suggesting a significantly lower amount of severe haze pollution during APEC. Indeed, 93% of the time during APEC, the NR-PM_1 level was lower than 60 μg m^{-3}, whereas 49% of the time before APEC exceeded such a concentration level. These results indicate that the air pollution was substantially more severe before APEC. The average mass concentration of NR-PM_1 was 24.1 μg m^{-3} during APEC, which is 63% lower than the 65.1 μg m^{-3} recorded before APEC (Fig. 6). This result demonstrates a significant reduction of PM during APEC due to emission controls and better weather conditions including higher WS and lower RH. However, the bulk NR-PM_1 composition was rather similar before and during APEC, both of which were dominated by organics, 46% versus 47%, followed by nitrate at 27% versus 29% and sulfate at 14% versus 10% (Fig. 6). The lower sulfate contribution during APEC might due to the lower RH, leading to less production of sulfate. These results highlight that the emission controls during APEC did not significantly affect the regional aerosol bulk composition, although the mass concentrations of precursors and aerosol species were reduced substantially. One possible explanation is the synergetic control of various precursors such as SO_2, NO_x, and volatile organic compounds (VOCs) over a regional scale during APEC. Our results clearly imply that synergetic controls of the emissions of precursors over a regional scale are efficient for mitigating air pollution in North China.

3.2.2 Diurnal variations

The diurnal variations of meteorological variables, NR-PM_1 species, and OA components before and during APEC are presented in Fig. 7. The diurnal cycles of meteorological conditions were overall similar before and during APEC except for lower temperatures and RH during APEC. The WS during APEC was consistently higher than that before APEC, particularly in the morning (04:00–12:00) and evening (18:00–22:00). Although the WD during APEC was dominantly from the northwest at night and shifted to the south during the day, it was mainly from the south before APEC (Fig. 2c).

412 The total NR-PM_1 showed pronounced diurnal variation with two peaks in early
413 afternoon (12:00–14:00) and late evening (20:00–22:00) that were dominantly
414 influenced by organics. By checking the diurnal cycles of the OA factors, we
415 concluded that the two peaks occurring at meal times are mainly attributed to primary
416 emissions such as cooking-related activities and traffic emissions (Allan et al.,
417 2010;Sun et al., 2011;Sun et al., 2012a). Compared with the diurnal cycles of OA
418 previously observed at the ground site in Beijing (Sun et al., 2012a), the two peaks of
419 organics were considerably smaller. This result indicates that local source emissions
420 can be vertically mixed above the urban canopy but at substantially reduced
421 concentrations. Our results also demonstrate that sampling above the urban canopy is
422 less influenced by local source emissions and can be more representative over a
423 regional scale.
424 SIA and OOA showed similar diurnal patterns before and during APEC, all of
425 which were characterized by gradual increases during the day. These results indicate
426 that their diurnal cycles were driven by similar formation mechanisms before and
427 during APEC such as photochemical processing and daytime vertical mixing. Higher
428 concentrations of secondary species were also observed at night, which might have
429 been associated with a shallower boundary layer height (Sun et al., 2012a). It should
430 be noted that all secondary species showed relatively constant background
431 concentrations, indicating that a major fraction was likely from regional transport. SIA
432 and OOA during APEC showed substantial reductions (45–74%) throughout the day
433 compared with those before APEC, indicating that regional emission controls played a
434 significant role in reducing secondary species during APEC, although the lower RH
435 and higher WS were also important. Moreover, a higher reduction percentage was
436 observed between 04:00 and 12:00, when higher mountain–valley breezes occurring
437 routinely during APEC cleaned the air pollutants more efficiently.
438 The diurnal cycles of chloride showed some differences before and during APEC.
439 Although it was relatively flat during APEC, chloride showed a clear decrease in the
440 afternoon before APEC, likely due to the evaporative loss and dilution effects
441 associated with higher *T* and the elevated boundary layer (Sun et al., 2012a). The

diurnal cycle of HOA showed overall lower concentration during the day except for a pronounced noon peak before and during APEC. Considering that the peak time corresponds to lunch time, we concluded that it was attributed mainly to local cooking sources. In addition, a more significant reduction in evening peak of HOA was observed during APEC. One explanation is that controls of heavy-duty vehicles (HDV) and heavy-duty diesel trucks (HDDT) decreased the HOA emissions at night during APEC.

3.2.3 Particle acidity

Particle acidity is a key parameter that influences aerosol toxicity, hygroscopic growth, and heterogeneous reactions (Sun et al., 2010). In this study, we evaluated aerosol particle acidity by using the ratio of measured NH_4^+ ($NH_4^+_{meas}$) to predicted NH_4^+ ($NH_4^+_{pred}$), which requires full neutralization of SO_4^{2-}, NO_3^-, and Cl^-: $NH_4^+_{pred} = 18 \times (2 \times SO_4^{2-}/96 + NO_3^-/62 + Cl^-/35.5)$ (Zhang et al., 2007a). Lower $NH_4^+_{meas}/NH_4^+_{pred}$ indicates greater aerosol particle acidity. As shown in Fig. 8, $NH_4^+_{meas}$ strongly correlated with $NH_4^+_{pred}$ before and during APEC (r^2 = 0.95 and 0.91, respectively), with regression slopes of 0.56 and 0.62, respectively. Slopes less than 1 indicate that aerosol particles above the urban canopy were acidic both before and during APEC. It should be noted that we might overestimate the particle acidity by counting all chloride as NH_4Cl. As indicated by the prominent *m/z* 60 in HOA spectrum, biomass burning could be an important source of primary aerosol at 260 m. Considering that chloride from biomass burning emissions could exist in the form of KCl, the approach recommended by Zhang et al. (2007a) would overestimate the predicted NH_4^+ and hence the aerosol particle acidity. Compared with the ground site measurement, $NH_4^+_{meas}/NH_4^+_{pred}$ = 0.75 and 0.80 for the periods before and during APEC, respectively, aerosol particles were more acidic above the urban canopy. One reason is that the concentration of SO_2 was higher above the urban canopy than that at the ground site (Meng et al., 2008). Another possible explanation is that the NH_3 from traffic emissions (Li et al., 2006;Meng et al., 2011) can neutralize more secondary inorganic aerosol near the ground level. Moreover, we detected a slight decrease in particle acidity during APEC, which is consistent with the slightly higher reduction of

sulfate than other inorganic species. One reason is likely the slightly greater reduction of SO_2 than other gaseous precursors during APEC. It is also possible that the lower RH during APEC decreased the aqueous-phase formation of sulfate and hence decreased particle acidity. Overall, the slight change in aerosol particle acidity revealed that the joint emission controls appear to have not affected the particle acidity significantly over regional scales, which is consistent with the small changes in aerosol composition before and during APEC.

3.2.4 Meteorological effects

Meteorological parameters contribute the largest uncertainties in evaluating the effects of emission controls on PM reduction. Here we compared the variations of aerosol species as a function of RH and WS before and during APEC. At low RH levels (<40%), all aerosol species appeared to increase linearly as a function of RH in both periods at similar rates of increase. Moreover, the mass concentrations of aerosol species were slightly lower during APEC than those before the summit, indicating small reductions in aerosol species during APEC. By checking the air mass trajectories (Fig. S~~53~~), we determined that the low RH periods were mainly associated with the air masses from the north/northwest where fewer emission controls were implemented during APEC. This finding explains the small reductions in aerosol species (~22%) during APEC under the same RH conditions. However, the variations in aerosol species showed substantially different behaviors as a function of RH at high RH levels (>40%) before and during APEC. Whereas most aerosol species continued to linearly increase as function of RH before APEC, they remained relatively constant and even showed deceases during APEC. As a result, significant reductions in aerosol species at high RH levels were observed during APEC. The air masses during high RH periods were found to be dominantly from the south/southeast where strict emission controls were implemented such as Hebei, Tianjin, and Shandong provinces. These results clearly indicate that emission controls played a major role in PM reduction during APEC and that the control effects tended to be more efficient under higher RH periods. The primary HOA and chloride showed decreases when the RH was >60%, indicating that humidity has a significantly lower impact on primary

aerosols than secondary components at high RH levels.

The mass concentrations of aerosol species showed a strong dependence on WS before and during APEC. For example, the total NR-PM_1 mass was decreased by ~80% from ~100 μg m^{-3} to < 20 μg m^{-3} as WS increased to 7 m s^{-1} before APEC. These results indicate that wind is efficient in cleaning air pollutants in Beijing, which is consistent with previous conclusions (Han et al., 2009;Sun et al., 2013c). In comparison, the decreasing rates of aerosol species as a function of WS were lower during APEC. As a result, aerosol species showed the largest concentration differences before and during APEC in periods with low WS. As indicated by the wind increase plots in Fig. 10, low and high WS were mainly associated with southern/southeastern and northern/northwestern winds, respectively. These results further indicate that larger reductions of aerosol species occurred in Beijing when air masses were from the south. ~~Our results also demonstrate that emission controls in surrounding regions to the south of Beijing should be taken as a priority for mitigation of air pollution in Beijing.~~

3.2.5 Back trajectory analysis

Figure 11 presents the average chemical composition of NR-PM_1, corresponding to four clusters before and during APEC, determined from the cluster analysis of back trajectories (Draxler and Hess, 1997). The air masses before APEC were predominantly from the south/southeast at 54% of the time (C1 in Fig. 11a), and the aerosol loading was the highest (96.7 μg m^{-3}) among the clusters. Comparatively, the northwesterly clusters (C3 and C4 in Fig. 11a) presented significantly lower aerosol loadings at 8.3 μg m^{-3} and 3.5 μg m^{-3}, respectively, with fewer frequencies of 14% and 11%, respectively. Such large differences in aerosol loadings between the northerly and southerly air masses are consistent with the spatial distributions of anthropogenic emissions such as SO_2, NO_x, and BC (Zhang et al., 2007b;Lu et al., 2011). Although the areas to the north/northwest of Beijing are relatively clean with low emissions of anthropogenic primary pollutants, the south/southeast regions are characterized by substantially higher emissions. In addition, 21% of the air masses originated from the west and showed moderately high NR-PM_1 mass at 55.4 μg m^{-3}.

532 It should be noted that the air masses from the south were often stagnant, as indicated
533 by their shorter trajectories, which played an important role in facilitating the
534 accumulation of pollutants. The aerosol composition varied significantly among four
535 clusters, reflecting the variety in chemical characteristics of aerosol particles from
536 different source regions. The aerosol particle composition from the southeastern and
537 western clusters (C1 and C2) were dominated by nitrate at 27% and 30% and OOA at
538 26% and 32%, respectively, with considerable contribution from sulfate at 14% and
539 10%, respectively. These results elucidate the dominant roles of nitrate and OOA in
540 severe PM pollution before APEC, which differs significantly from previous studies
541 reporting that sulfate was generally more prevalent than nitrate (Huang et al.,
542 2014;Sun et al., 2014). These results also highlight a very different pollution
543 characteristic during the late fall season from that in winter. In comparison, the nitrate
544 contributions were significantly lower, at 17% and 8%, in the two northwestern
545 clusters (C3 and C4) associated with an enhanced contribution of sulfate at 19% and
546 21%, respectively. Moreover, the cleanest cluster (C4) showed a dominant
547 contribution of organics at 64%, indicating the important role of organics during clean
548 periods (Sun et al., 2010;Sun et al., 2013c).
549 The air masses during APEC showed changes, particularly the increases in
550 frequency of two northwestern clusters (C1 and C4), which was 40% of the time
551 compared with 25% before APEC (Fig. 11b). These two clusters showed similar bulk
552 aerosol compositions to those before APEC yet with reductions of the total NR-PM_1
553 mass loading at nearly 40–50%. The air masses during APEC were dominated by
554 cluster 3 (C3 in Fig. 11b). Although C3 originated from the north of Beijing, it
555 circulated around the south of Beijing including Baoding, a polluted city in Hebei
556 province, before arriving at the sampling site. As a result, C3 presented the highest
557 aerosol mass loading, at 44.0 μg m^{-3}, composed primarily of nitrate and OOA at 30%
558 and 29%, respectively. Moreover, cluster 2 (C2 in Fig. 11b), originating from the
559 northwest, showed a similar aerosol composition yet had an ~50% decrease in total
560 mass compared to C3. One explanation is that air masses in C2 passed through the
561 western Beijing, where is relatively cleaner than the southeastern regions. As shown

in Fig. 11, similar clusters before and during APEC showed ubiquitous reductions in NR-PM_1 mass during APEC, indicating that emission controls played an important role in PM reduction. Moreover, the decreases in frequency of southern/southeastern air masses during APEC also helped to alleviate the PM level for the entire period, thus achieving the "APEC blue" effect. Emission controls in surrounding regions south of Beijing should be taken as a priority for mitigation of air pollution in Beijing.

3.3 Vertical differences: insights into emission controls and boundary layer dynamics

Figure 12 shows a comparison of the time series of NR-PM_1 species between 260 m and the ground level for the entire study. All submicron species showed overall similar variations at the two different heights, indicating their relatively similar sources and evolution processes. However, large vertical differences in aerosol composition were also frequently observed, illustrating complex vertical gradients of aerosol species caused by multiple factors such as local emissions, regional transport, and boundary layer dynamics. The average compositional differences before and during APEC are shown in Fig. 13. Although the concentration difference in NR-PM_1 was close before and during APEC at 12.1 μg m^{-3} and 14.1 μg m^{-3}, respectively, the composition differed significantly. SIA dominated the compositional difference before APEC, together accounting for 95% of the total NR-PM_1 mass. In comparison, organics and chloride showed minor vertical differences (<5%). These results indicate different sources and formation mechanisms between SIA and organic aerosol. During APEC, the compositional difference was dominated by organics, accounting for 68% on average, and the contributions of SIA were largely reduced at 25%. These results suggest that emission controls over regional scales affect the composition differences between ground level and the urban canopy. As discussed in section 3.2 and by Xu et al. (2015), secondary species including SIA and SOA showed significant reductions at both ground level and 260 m during APEC as a result of emission controls. Although primary OA showed similar reductions as those of SOA above the urban canopy, the changes remained small near the ground level. Thus, the largest organic difference during APEC was mainly caused by local primary source emissions.

The vertical differences in aerosol composition also varied largely among different haze episodes. As indicated in Fig. 12 and Table 1, Ep3 presented the smallest vertical differences for all aerosol species, indicating a well-mixed layer below 260 m. The WS was consistently low at <2.5 m s^{-1} across the different heights, and the WD was predominantly from the south during Ep3. Moreover, the vertical profiles of extinction showed an evident reduction in pollution from ~2 km to the ground on October 28, leading to the formation of Ep3 (Fig. S64). Such boundary layer dynamics would produce a well-mixed layer in the lower atmosphere, leading to minor chemical differences between the ground level and 260 m.

Comparatively, the vertical evolution of Ep2 differed significantly (Fig. 14a). The mass concentrations of all aerosol species between the ground level and 260 m were similar during the formation stage of Ep2, from October 23 to 9:00 October 24. However, although aerosol species near the ground level showed large increases after 9:00 on October24, they remained relatively constant at 260 m, leading to the largest vertical concentration gradients among five episodes. The average NR-PM_1 at 260 m was 143.4 μg m^{-3}, which is 38% lower than that at the ground site. By checking the vertical profiles of meteorological variables, we observed a clear temperature inversion between 120 m and 160 m that formed during 0:00–9:00 on October 24. Such a temperature inversion formed a stable layer below ~200 m and inhibited the vertical mixing of air pollutants between the ground and 260 m. In addition, the stagnant meteorological conditions as indicated by low WS and high RH further facilitated the accumulation of ground pollution. It should be noted that the aqueous-phase processing, most likely fog processing under the high RH conditions (often > 90%) during this stage, also played an important role in the increase of SIA, particularly sulfate. This finding is also supported by the significant increase of SOR during this stage (Fig. 3).

The evolution of the severe Ep2 was terminated at approximately 0:00 on October 26 when the WD changed from south to northwest. Although the mass concentrations of aerosol species at 260 m began to show rapid decreases at that time, the concentration at the ground site decreased significantly after 4 hours. The different

622 cleaning processes between 260 m and the ground level are closely linked to the
623 vertical profiles of meteorological variables. As indicated in Fig. 14a, a strong
624 temperature inversion below 320 m was observed during the cleaning period, which
625 resulted in a significantly higher WS and lower RH at 260 m than those at ground
626 level. Indeed, both WS and RH showed clear shears during the cleaning period,
627 suggesting a gradual interaction between the northern air mass and boundary pollution
628 from top to bottom. Such an interacting mechanism resulted in a time lag of
629 approximately 4 h in cleaning the pollutants at ground level over that at 260 m.
630 Similar interactions between boundary layer dynamics and aerosol pollution were also
631 observed on November 1, 5, and 11.

632 The evolution of vertical differences during APEC differed from those in three
633 episodes before APEC. As shown in Fig. 14b, frequent mountain–valley breezes were
634 observed during November 8–11 (APEC2). The northwest mountain–valley breeze
635 began routinely at approximately midnight and dissipated at approximately noon. The
636 NR-PM_1 aerosol species showed direct responses to the mountain–valley breeze,
637 which was characterized by similar routine diurnal cycles. All aerosol species began
638 to decrease at midnight because the cleaning effects of mountain–valley breeze
639 reached minimum concentrations at noon, then increased continuously when the WD
640 changed to south. The mountain–valley breeze also caused a unique diurnal cycle of
641 vertical differences. As shown in Fig. 14b, aerosol species were well mixed within the
642 lower boundary layer between 12:00 and 16:00, and the concentrations between 260
643 m and the ground level were similar. However, the differences in concentration began
644 to increase when the boundary layer height decreased after sunset at ~18:00, and the
645 differences were maximum at midnight when the NR-PM_1 mass approached 100 μg
646 m^{-3}. A detailed check of the evolution of aerosol species showed that such vertical
647 differences in NR-PM_1 were caused mainly by organics from local primary sources
648 (Xu et al. in preparation; Fig. 12). These results indicate that local source emissions
649 played a more important role in PM pollution near ground level during APEC. The
650 concentration differences in NR-PM_1 began to decrease with the occurrence of the
651 mountain–valley breeze and reached a minimum at noon. Our results revealed the

important role of mountain–valley breeze in affecting the boundary layer structure and reducing the daytime PM levels during APEC. It was estimated that the mountain–valley breeze caused a reduction in NR-PM_1 concentration of approximately 50 μg m^{-3} at the ground site during the day on November 10–11 (Fig. 14b). Therefore, our results illustrated that the achievement of "APEC blue" was also due partly to meteorological effects, particularly the mountain–valley breeze, in addition to emission controls.

4. Conclusions

We have presented a detailed characterization of aerosol particle composition and sources above the urban canopy in Beijing from October 10 to November 12, 2014. This study is unique because it examines strict emission controls implemented during the 2014 APEC summit and synchronous real-time measurements of aerosol particle composition at 260 m and that near the ground level obtained by two aerosol mass spectrometers. The NR-PM_1 composition above the urban canopy was dominated by organics at 46%, followed by nitrate at 27% and sulfate at 13%. The high contribution of nitrate and high NO_3^-/SO_4^{2-} mass ratios illustrate the important role of nitrate in PM pollution during the study period. This result has significant implications that NO_x emission controls should be prioritized for the mitigation of air pollution in Beijing, particularly in non-heating seasons with low SO_2 precursors. The OA above the urban canopy was dominated by OOA at 61% and included HOA at 39%. Different from that at the ground site, HOA correlated moderately with OOA above the urban canopy, indicating similar sources likely through regional transport.

With the implementation of emission controls, the mass concentrations of aerosol species were shown to have decreased significantly by 40–80% during APEC, whereas the bulk aerosol composition was relatively similar before and during APEC. Organics were dominant before and during the summit, at 46% versus 47%, respectively, followed by nitrate at 27% versus 29% and sulfate at 14% versus 10%, respectively. Our results suggest that synergetic controls of various precursors such as SO_2, NO_x, and VOCs over a regional scale would not significantly affect regional

aerosol bulk composition, although the mass concentrations would be reduced substantially. By linking aerosol compositions and sources to meteorological conditions, we determined that meteorological parameters, particularly mountain–valley breezes, played an important role in suppressing PM growth and hence reducing PM levels during APEC. Our results elucidated that the good air quality in Beijing during APEC was the combined result of emission controls and meteorological effects, with the former playing the dominant role. We further investigated the vertical evolution of aerosol particle composition by comparing the aerosol chemistry between the ground level and 260 m. We observed very complex vertical differences during the formation and evolution of severe haze episodes that were closely related to aerosol sources (local versus regional) and boundary layer dynamics. Although a stable *T* inversion layer between 120 m and 160 m associated with stagnant meteorology caused ~~cause~~ higher concentrations of aerosol species at the ground site, the interaction of boundary layer dynamics and aerosol chemistry during the cleaning processes resulted in a lag time of approximately 4 h in cleaning pollutants near the ground level over those occurring above the urban canopy.

Acknowledgements

This work was supported by the National Key Project of Basic Research (2014CB447900), the Strategic Priority Research Program (B) of the Chinese Academy of Sciences (XDB05020501), the Key Research Program of the Chinese Academy of Sciences (KJZD-EW-TZ-G06-01-0), and the Special Fund for Environmental Protection Research in the Public Interest (201409001).

References

Aiken, A. C., Salcedo, D., Cubison, M. J., Huffman, J. A., DeCarlo, P. F., Ulbrich, I. M., Docherty, K. S., Sueper, D., Kimmel, J. R., Worsnop, D. R., Trimborn, A., Northway, M., Stone, E. A., Schauer, J. J., Volkamer, R. M., Fortner, E., de Foy, B., Wang, J., Laskin, A., Shutthanandan, V., Zheng, J., Zhang, R., Gaffney, J., Marley, N. A., Paredes-Miranda, G., Arnott, W. P., Molina, L. T., Sosa, G., and Jimenez, J. L.: Mexico City aerosol analysis during MILAGRO using high resolution aerosol mass spectrometry at the urban supersite (T0) - Part 1: Fine particle composition and organic source apportionment, Atmos. Chem. Phys., 9, 6633-6653, 2009.

Allan, J., Williams, P., Morgan, W., Martin, C., Flynn, M., Lee, J., Nemitz, E., Phillips, G., Gallagher, M., and Coe, H.: Contributions from transport, solid fuel burning and cooking to primary organic aerosols in two UK cities, Atmos. Chem. Phys., 10, 647-668, 2010.

Arimoto, R., Duce, R., Savoie, D., Prospero, J., Talbot, R., Cullen, J., Tomza, U., Lewis, N., and Ray, B.: Relationships among aerosol constituents from Asia and the North Pacific during PEM‐West A, Journal of Geophysical Research: Atmospheres (1984–2012), 101, 2011-2023, 1996.

Budisulistiorini, S., Canagaratna, M., Croteau, P., Baumann, K., Edgerton, E., Kollman, M., Ng, N., Verma, V., Shaw, S., and Knipping, E.: Intercomparison of an Aerosol Chemical Speciation Monitor (ACSM) with ambient fine aerosol measurements in downtown Atlanta, Georgia, Atmospheric Measurement Techniques, 7, 1929-1941, 2014.

Draxler, R. R., and Hess, G.: Description of the HYSPLIT4 modeling system, Air Resources Laboratory, Silver Spring, Maryland, 1997.

Guinot, B., Roger, J.-C., Cachier, H., Pucai, W., Jianhui, B., and Tong, Y.: Impact of vertical atmospheric structure on Beijing aerosol distribution, Atmos. Environ., 40, 5167-5180, 2006.

Guo, S., Hu, M., Zamora, M. L., Peng, J., Shang, D., Zheng, J., Du, Z., Wu, Z., Shao, M., and Zeng, L.: Elucidating severe urban haze formation in China, Proc. Natl. Acad. Sci. U.S.A., 111, 17373-17378, 2014.

Han, S., Kondo, Y., Oshima, N., Takegawa, N., Miyazaki, Y., Hu, M., Lin, P., Deng, Z., Zhao, Y., and Sugimoto, N.: Temporal variations of elemental carbon in Beijing, Journal of Geophysical Research: Atmospheres (1984–2012), 114, D23202, doi:23210.21029/22009JD012027, 2009.

Hu, W. W., Hu, M., Yuan, B., Jimenez, J. L., Tang, Q., Peng, J., Hu, W., Shao, M., Wang, M., and Zeng, L.: Insights on organic aerosol aging and the influence of coal combustion at a regional receptor site of central eastern China, Atmos. Chem. Phys, 13, 095, 2013.

Huang, K., Zhuang, G., Lin, Y., Fu, J., Wang, Q., Liu, T., Zhang, R., Jiang, Y., Deng, C., and Fu, Q.: Typical types and formation mechanisms of haze in an Eastern Asia megacity, Shanghai, Atmos. Chem. Phys., 12, 105-124, 2012a.

Huang, R. J., Zhang, Y., Bozzetti, C., Ho, K. F., Cao, J. J., Han, Y., Daellenbach, K. R., Slowik, J. G., Platt, S. M., Canonaco, F., Zotter, P., Wolf, R., Pieber, S. M., Bruns,

749 E. A., Crippa, M., Ciarelli, G., Piazzalunga, A., Schwikowski, M., Abbaszade, G.,
750 Schnelle-Kreis, J., Zimmermann, R., An, Z., Szidat, S., Baltensperger, U., El
751 Haddad, I., and Prevot, A. S.: High secondary aerosol contribution to particulate
752 pollution during haze events in China, Nature, 514, 218-222,
753 10.1038/nature13774, 2014.
754 Huang, X.-F., He, L.-Y., Hu, M., Canagaratna, M., Sun, Y., Zhang, Q., Zhu, T., Xue,
755 L., Zeng, L.-W., and Liu, X.-G.: Highly time-resolved chemical characterization
756 of atmospheric submicron particles during 2008 Beijing Olympic Games using an
757 Aerodyne High-Resolution Aerosol Mass Spectrometer, Atmos. Chem. Phys., 10,
758 8933-8945, 2010.
759 Huang, X.-F., He, L.-Y., Xue, L., Sun, T.-L., Zeng, L.-W., Gong, Z.-H., Hu, M., and
760 Zhu, T.: Highly time-resolved chemical characterization of atmospheric fine
761 particles during 2010 Shanghai World Expo, Atmos. Chem. Phys., 12, 4897-4907,
762 2012b.
763 Huang, X.-F., Xue, L., Tian, X.-D., Shao, W.-W., Sun, T.-L., Gong, Z.-H., Ju, W.-W.,
764 Jiang, B., Hu, M., and He, L.-Y.: Highly time-resolved carbonaceous aerosol
765 characterization in Yangtze River Delta of China: Composition, mixing state and
766 secondary formation, Atmos. Environ., 64, 200-207, 2013.
767 Huang, X. F., He, L. Y., Hu, M., Canagaratna, M. R., Kroll, J. H., Ng, N. L., Zhang, Y.
768 H., Lin, Y., Xue, L., Sun, T. L., Liu, X. G., Shao, M., Jayne, J. T., and Worsnop, D.
769 R.: Characterization of submicron aerosols at a rural site in Pearl River Delta of
770 China using an Aerodyne High-Resolution Aerosol Mass Spectrometer, Atmos.
771 Chem. Phys., 11, 1865-1877, 10.5194/acp-11-1865-2011, 2011.
772 Jia, Y., Rahn, K. A., He, K., Wen, T., and Wang, Y.: A novel technique for quantifying
773 the regional component of urban aerosol solely from its sawtooth cycles, J.
774 Geophys. Res., 113, D21309, 10.1029/2008jd010389, 2008.
775 Jimenez, J., Canagaratna, M., Donahue, N., Prevot, A., Zhang, Q., Kroll, J., DeCarlo,
776 P., Allan, J., Coe, H., and Ng, N.: Evolution of organic aerosols in the atmosphere,
777 Science, 326, 1525-1529, 2009.
778 Li, W., Shao, L., and Buseck, P.: Haze types in Beijing and the influence of
779 agricultural biomass burning, Atmos. Chem. Phys., 10, 8119-8130, 2010.
780 Li, Y., Schwab, J. J., and Demerjian, K. L.: Measurements of ambient ammonia using
781 a tunable diode laser absorption spectrometer: Characteristics of ambient
782 ammonia emissions in an urban area of New York City, J. Geophys. Res., 111,
783 D10S02, 10.1029/2005jd006275, 2006.
784 Li, Y., Lee, B., Su, L., Fung, J., and Chan, C.: Seasonal characteristics of fine
785 particulate matter (PM) based on high-resolution time-of-flight aerosol mass
786 spectrometric (HR-ToF-AMS) measurements at the HKUST Supersite in Hong
787 Kong, Atmos. Chem. Phys., 15, 37-53, 2015.
788 Lu, Z., Zhang, Q., and Streets, D. G.: Sulfur dioxide and primary carbonaceous
789 aerosol emissions in China and India, 1996–2010, Atmos. Chem. Phys., 11,
790 9839-9864, 10.5194/acp-11-9839-2011, 2011.
791 Matthew, B. M., Middlebrook, A. M., and Onasch, T. B.: Collection efficiencies in an
792 Aerodyne Aerosol Mass Spectrometer as a function of particle phase for

laboratory generated aerosols, Aerosol Sci. Tech., 42, 884-898, 2008.
Meng, Z., Ding, G., Xu, X., Xu, X., Yu, H., and Wang, S.: Vertical distributions of SO 2 and NO 2 in the lower atmosphere in Beijing urban areas, China, Sci. Total Environ., 390, 456-465, 2008.
Meng, Z., Lin, W., Jiang, X., Yan, P., Wang, Y., Zhang, Y., Jia, X., and Yu, X.: Characteristics of atmospheric ammonia over Beijing, China, Atmos. Chem. Phys., 11, 6139-6151, 2011.
Middlebrook, A. M., Bahreini, R., Jimenez, J. L., and Canagaratna, M. R.: Evaluation of composition-dependent collection efficiencies for the aerodyne aerosol mass spectrometer using field data, Aerosol Sci. Tech., 46, 258-271, 2012.
Mohr, C., Huffman, J. A., Cubison, M. J., Aiken, A. C., Docherty, K. S., Kimmel, J. R., Ulbrich, I. M., Hannigan, M., and Jimenez, J. L.: Characterization of primary organic aerosol emissions from meat cooking, trash burning, and motor vehicles with high-resolution aerosol mass spectrometry and comparison with ambient and chamber observations, Environ. Sci. Technol., 43, 2443-2449, 2009.
Ng, N. L., Herndon, S. C., Trimborn, A., Canagaratna, M. R., Croteau, P., Onasch, T. B., Sueper, D., Worsnop, D. R., Zhang, Q., and Sun, Y.: An Aerosol Chemical Speciation Monitor (ACSM) for routine monitoring of the composition and mass concentrations of ambient aerosol, Aerosol Sci. Tech., 45, 780-794, 2011.
Paatero, P., and Tapper, U.: Positive matrix factorization: A non‐negative factor model with optimal utilization of error estimates of data values, Environmetrics, 5, 111-126, 1994.
Parworth, C., Fast, J., Mei, F., Shippert, T., Sivaraman, C., Tilp, A., Watson, T., and Zhang, Q.: Long-term measurements of submicrometer aerosol chemistry at the Southern Great Plains (SGP) using an Aerosol Chemical Speciation Monitor (ACSM), Atmos. Environ., 106, 43-55, 2015.
Petit, J.-E., Favez, O., Sciare, J., Crenn, V., Sarda-Estève, R., Bonnaire, N., Močnik, G., Dupont, J.-C., Haeffelin, M., and Leoz-Garziandia, E.: Two years of near real-time chemical composition of submicron aerosols in the region of Paris using an Aerosol Chemical Speciation Monitor (ACSM) and a multi-wavelength Aethalometer, Atmos. Chem. Phys., 15, 2985-3005, 2015.
Pope III, C. A., Ezzati, M., and Dockery, D. W.: Fine-particulate air pollution and life expectancy in the United States, New England Journal of Medicine, 360, 376-386, 2009.
Quinn, P., Bates, T., Coffman, D., Onasch, T., Worsnop, D., Baynard, T., De Gouw, J., Goldan, P., Kuster, W., and Williams, E.: Impacts of sources and aging on submicrometer aerosol properties in the marine boundary layer across the Gulf of Maine, J. Geophys. Res.: Atmos. (1984–2012), 111, D23S36, doi:10.1029/2006jd007582, 2006.
Sun, J., Zhang, Q., Canagaratna, M. R., Zhang, Y., Ng, N. L., Sun, Y., Jayne, J. T., Zhang, X., Zhang, X., and Worsnop, D. R.: Highly time-and size-resolved characterization of submicron aerosol particles in Beijing using an Aerodyne Aerosol Mass Spectrometer, Atmos. Environ., 44, 131-140, 2010.
Sun, Y.-L., Zhang, Q., Schwab, J., Demerjian, K., Chen, W.-N., Bae, M.-S., Hung,

H.-M., Hogrefe, O., Frank, B., and Rattigan, O.: Characterization of the sources and processes of organic and inorganic aerosols in New York city with a high-resolution time-of-flight aerosol mass apectrometer, Atmos. Chem. Phys., 11, 1581-1602, 2011.

Sun, Y., Zhuang, G., Tang, A., Wang, Y., and An, Z.: Chemical characteristics of PM2. 5 and PM10 in haze-fog episodes in Beijing, Environ. Sci. Technol., 40, 3148-3155, 2006.

Sun, Y., Wang, Y., and Zhang, C.: Measurement of the vertical profile of atmospheric SO 2 during the heating period in Beijing on days of high air pollution, Atmos. Environ., 43, 468-472, 2009.

Sun, Y., Wang, Z., Dong, H., Yang, T., Li, J., Pan, X., Chen, P., and Jayne, J. T.: Characterization of summer organic and inorganic aerosols in Beijing, China with an Aerosol Chemical Speciation Monitor, Atmos. Environ., 51, 250-259, 2012a.

Sun, Y., Zhang, Q., Schwab, J., Yang, T., Ng, N., and Demerjian, K.: Factor analysis of combined organic and inorganic aerosol mass spectra from high resolution aerosol mass spectrometer measurements, Atmos. Chem. Phys., 12, 8537-8551, 2012b.

Sun, Y., Song, T., Tang, G., and Wang, Y.: The vertical distribution of PM 2.5 and boundary-layer structure during summer haze in Beijing, Atmos. Environ., 74, 413-421, 2013a.

Sun, Y., Wang, Z., Fu, P., Jiang, Q., Yang, T., Li, J., and Ge, X.: The impact of relative humidity on aerosol composition and evolution processes during wintertime in Beijing, China, Atmos. Environ., 77, 927-934, 2013b.

Sun, Y., Wang, Z., Fu, P., Yang, T., Jiang, Q., Dong, H., Li, J., and Jia, J.: Aerosol composition, sources and processes during wintertime in Beijing, China, Atmos. Chem. Phys., 13, 4577-4592, 2013c.

Sun, Y. L., Jiang, Q., Wang, Z., Fu, P., Li, J., Yang, T., and Yin, Y.: Investigation of the sources and evolution processes of severe haze pollution in Beijing in January 2013, J. Geophys. Res.: Atmos., 119, 4380-4398, 2014.

Sun, Y., Du, W., Wang, Q., Zhang, Q., Chen, C., Chen, Y., Chen, Z., Fu, P., Wang, Z., Gao, Z., and Worsnop, D.: Real-Time Characterization of Aerosol Particle Composition above the Urban Canopy in Beijing: Insights into the Interactions between the Atmospheric Boundary Layer and Aerosol Chemistry, Environ. Sci. Technol., 49, 11340–11347, 10.1021/acs.est.5b02373, 2015.

Ting, M., Yue-Si, W., Jie, J., Fang-Kun, W., and Mingxing, W.: The vertical distributions of VOCs in the atmosphere of Beijing in autumn, Sci. Total Environ., 390, 97-108, 2008.

Ulbrich, I., Canagaratna, M., Zhang, Q., Worsnop, D., and Jimenez, J.: Interpretation of organic components from Positive Matrix Factorization of aerosol mass spectrometric data, Atmos. Chem. Phys., 9, 2891-2918, 2009.

Wang, Y., Zhang, Q. Q., He, K., Zhang, Q., and Chai, L.: Sulfate-nitrate-ammonium aerosols over China: response to 2000–2015 emission changes of sulfur dioxide, nitrogen oxides, and ammonia, Atmos. Chem. Phys., 13, 2635-2652, 10.5194/acp-13-2635-2013, 2013.

Xiao, R., Takegawa, N., Zheng, M., Kondo, Y., Miyazaki, Y., Miyakawa, T., Hu, M., Shao, M., Zeng, L., and Gong, Y.: Characterization and source apportionment of submicron aerosol with aerosol mass spectrometer during the PRIDE-PRD 2006 campaign, Atmos. Chem. Phys., 11, 6911-6929, 2011.

Xu, W., Sun, Y., Chen, C., Du, W., Han, T., Wang, Q., Fu, P., Wang, Z., Zhao, X., and Zhou, L.: Aerosol composition, oxidative properties, and sources in Beijing: results from the 2014 Asia-Pacific Economic Cooperation Summit study, Atmospheric Chemistry and Physics Discussions, 15, 23407-23455, 2015.

Zhang, J., Sun, Y., Liu, Z., Ji, D., Hu, B., Liu, Q., and Wang, Y.: Characterization of submicron aerosols during a month of serious pollution in Beijing, 2013, Atmos. Chem. Phys., 14, 2887-2903, 2014.

Zhang, Q., Worsnop, D., Canagaratna, M., and Jimenez, J.: Hydrocarbon-like and oxygenated organic aerosols in Pittsburgh: insights into sources and processes of organic aerosols, Atmos. Chem. Phys., 5, 3289-3311, 2005.

~~Zhang, Q., Jimenez, J., Canagaratna, M., Allan, J., Coe, H., Ulbrich, I., Alfarra, M., Takami, A., Middlebrook, A., and Sun, Y.: Ubiquity and dominance of oxygenated species in organic aerosols in anthropogenically - influenced Northern Hemisphere midlatitudes, Geophys. Res. Lett., 34, L13801, doi:10.1029/2007GL029979, 2007a.~~

Zhang, Q., Jimenez, J. L., Worsnop, D. R., and Canagaratna, M.: A case study of urban particle acidity and its effect on secondary organic aerosol, Environ. Sci. Technol., 41, 3213-3219, 2007a.

Zhang, Q., Streets, D. G., He, K., Wang, Y., Richter, A., Burrows, J. P., Uno, I., Jang, C. J., Chen, D., Yao, Z., and Lei, Y.: NOx emission trends for China, 1995-2004: The view from the ground and the view from space, J. Geophys. Res., 112, D22306, 10.1029/2007jd008684, 2007b.

Zhang, Q., Jimenez, J. L., Canagaratna, M. R., Ulbrich, I. M., Ng, N. L., Worsnop, D. R., and Sun, Y.: Understanding atmospheric organic aerosols via factor analysis of aerosol mass spectrometry: a review, Anal. Bioanal. Chem., 401, 3045-3067, 2011.

Zhang, Q., and Tie, X.: High solubility of SO2: evidence in an intensive fog event measured in the NCP region, China, Atmos. Chem. Phys. Discuss., 11, 2931-2947, 10.5194/acpd-11-2931-2011, 2011.

Zhang, Q., Meng, J., Quan, J., Gao, Y., Zhao, D., Chen, P., and He, H.: Impact of aerosol composition on cloud condensation nuclei activity, Atmos. Chem. Phys., 12, 3783-3790, 2012.

Zhang, W., Zhang, Y., Lv, Y., Li, K., and Li, Z.: Observation of atmospheric boundary layer height by ground-based LiDAR during haze days, Journal of Remote Sensing, 17, 981-992, 2013.

Zhang, Y., Tang, L., Wang, Z., Yu, H., Sun, Y., Liu, D., Qin, W., Canonaco, F., Prévôt, A., and Zhang, H.: Insights into characteristics, sources, and evolution of submicron aerosols during harvest seasons in the Yangtze River delta region, China, Atmos. Chem. Phys., 15, 1331-1349, 2015.

Zhao, X., Zhao, P., Xu, J., Meng, W., Pu, W., Dong, F., He, D., and Shi, Q.: Analysis

925 of a winter regional haze event and its formation mechanism in the North China
926 Plain, Atmos. Chem. Phys., 13, 5685-5696, 2013.
927

928 **Table 1.** Summary of average meteorological variables for different periods and the
929 mass differences of aerosol species between ground site and 260 m (= ground – 260
930 m).

	Before APEC				During APEC		
	Entire	Ep1	Ep2	Ep3	Entire	APEC1	APEC2
Meteorological Variables							
RH (%)	47.1	48.4	69.7	56.7	29.8	34.2	38.5
T (°C)	13.3	16.7	12.5	10.9	9.0	11.5	8.1
WS ($m\ s^{-1}$)	4.0	3.4	2.3	2.3	4.9	3.8	3.1
Mass Differences ($\mu g\ m^{-3}$)							
Org	0.7	0.3	4.5	-5.2	9.6	14.6	13.6
SO_4^{2-}	3.4	3.0	8.8	1.3	1.3	1.6	1.9
NO_3^-	4.3	4.5	10.9	0.8	0.7	1.0	1.0
NH_4^+	3.9	4.2	9.0	2.3	1.6	2.9	2.3
Cl^-	-0.1	0.0	-0.4	-0.2	1.0	1.7	1.5
NR-PM_1	12.1	12.0	32.8	-1.1	14.1	21.8	20.2

931

Figure captions:

Figure 1. Evolution of vertical profiles of (a) wind speed (WS) and (b) wind direction (WD) from the measurements of the Doppler wind lidar.The time series of NR-PM_1 (=Org + SO_4^{2-} + NO_3^- + NH_4^+ + Cl^-) is shown as the black line in (a). The shaded area refers to the APEC period (same for following figures).

Figure 2. Time series of (a) *T*, (b) RH, (c) WS and WD, (d) NR-PM_1 species (Org, SO_4^{2-}, NO_3^-, NH_4^+, and Cl^-), and (f) mass fraction of each species in NR-PM_1. Two clean periods and five haze episodes are marked in Fig. 2d for further discussions. ~~Note that t~~The meteorological parameters in this figure were all from the tower measurements.

Figure 3. Time series of (a) sulfur oxidation ratio (SOR), (b) ratio of NO_3^-/SO_4^{2-}, and (c) NR-PM_1. The SOR and NO_3^-/SO_4^{2-} were color coded by RH.

Figure 4. (a) Mass spectra of HOA and OOA, (b) diurnal variations of the mass concentration and mass fraction of HOA and OOA, (c) time series of HOA, OOA, and inorganic species (SO_4^{2-}, NO_3^-, Cl^-). The correlations of HOA and OOA with inorganic specie are also shown in the figure.

Figure 5. Submicron aerosol composition as a function of NR-PM_1 mass loadings (a) before APEC and (b) during APEC. The solide line shows the probability of NR-PM_1 mass.

Figure 6. Average chemical composition of NR-PM_1 before and during APEC, and also that of five haze episodes and two clean events marked in Fig. 2.

Figure 7. Diurnal variations of meteorological variables (*T*, RH, WS, and WD), NR-PM_1 species, and OA factors before and during APEC. The change rates during APEC (= (Before APEC –APEC)/ Before APEC × 100) are also marked as light gray in the figure.

Figure 8. Correlations between measured NH_4^+ and predicted NH_4^+ (= 18×(2×SO_4^{2-}/96 + NO_3^-/62 + Cl^-/35.5)) before and during APEC. The inset plot shows the correlations of measured NH_4^+ vs. predicted NH_4^+ at the ground site.

Figure 9. Variations of NR-PM_1 species and OA factors as a function of (a) RH and (b) WS before and during APEC. The RH and WS were from the tower measurements at 280 m.

Figure 10. Wind rose plots (a) before APEC and (b) during APEC.

Figure 11. The average NR-PM_1 composition for each cluster (a) before and (b) during APEC. The numbers on the pie charts refer to the average total NR-PM_1 mass for each cluster. In addition, the number of trajectories and its percentage to the total trajectories are also shown in the legends.

Figure 12. Comparisons of time series of total NR-PM_1 mass and NR-PM_1 species between 260 m and ground level.

Figure 13. Average chemical composition of the difference between ground level and 260 m (a) before APEC and (b) during APEC. The "1%" in the box indicates lower concentration of chloride at ground site than 260 m.

Figure 14. The evolution of vertical profiles of meteorological variables (WD, WS, RH, and *T*), and NR-PM_1 concentration at 260 m and ground site during two pollution

episodes (a) Ep2 and (b) APEC2. The vertical profiles of wind speed and wind direction were from the measurements of the Doppler wind lidar, and those of RH and *T* were from the tower measurements. The white areas in the figure indicate that the data were not available.

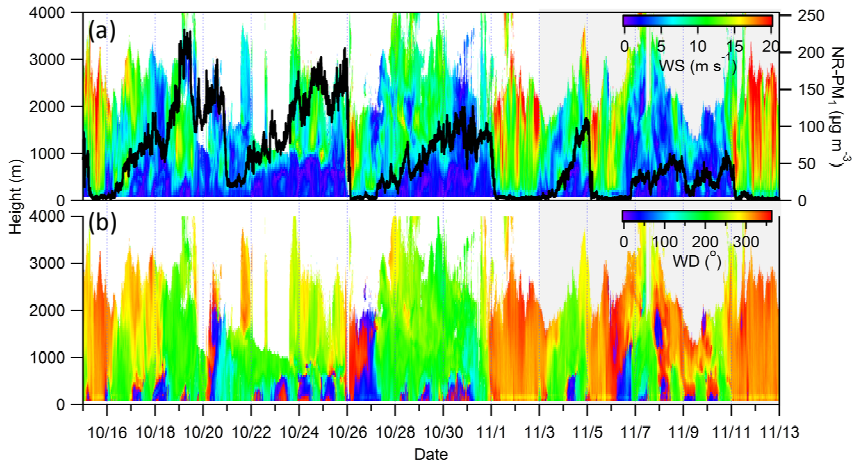

Figure 1. Evolution of vertical profiles of (a) wind speed (WS) and (b) wind direction (WD) from the measurements of the Doppler wind lidar. The time series of NR-PM_1 (= Org + SO_4^{2-} + NO_3^- + NH_4^+ + Cl^-) is shown as the black line in (a). The shaded area refers to the Asia–Pacific Economic Cooperation (APEC) summit period, which is the same in the following figures.

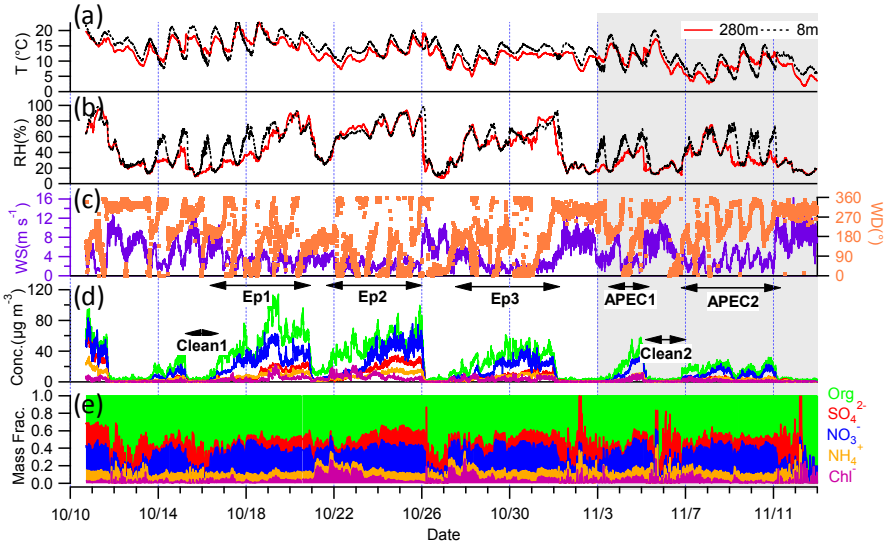

Figure 2. Time series of (a) temperature (*T*), (b) relative humidity (RH), (c) wind speed (WS) and wind direction (WD), (d) non-refractory submicron aerosol (NR-PM_1) species (Org, SO_4^{2-}, NO_3^-, NH_4^+, and Cl^-), and (f) mass fraction of each species in NR-PM_1. Two clean periods and five haze episodes are marked in Fig. 2d for further discussion. The meteorological parameters in this figure were all from the tower measurements.

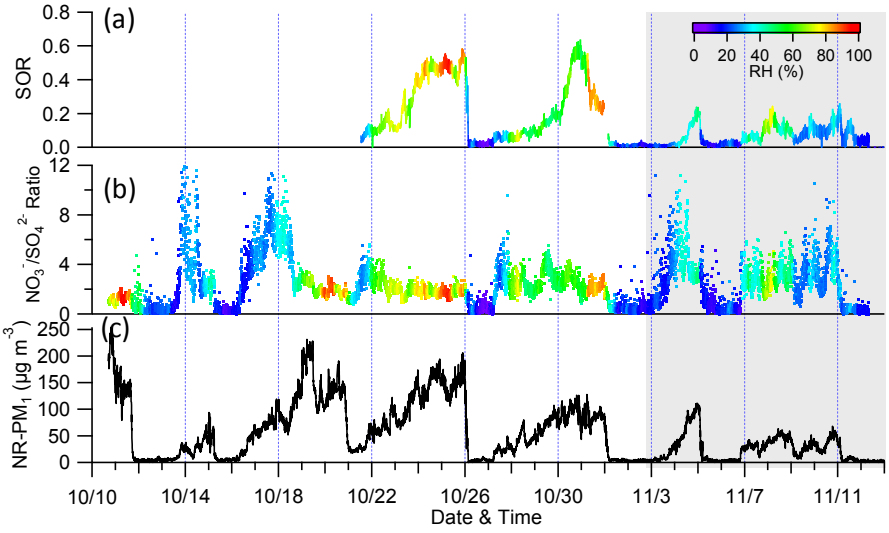

994

995 **Figure 3.** Time series of (a) sulfur oxidation ratio (SOR), (b) the ratio of NO_3^-/SO_4^{2-},
996 and (c) non-refractory submicron aerosol ($NR\text{-}PM_1$). The SOR and NO_3^-/SO_4^{2-} are
997 color coded by relative humidity (RH).

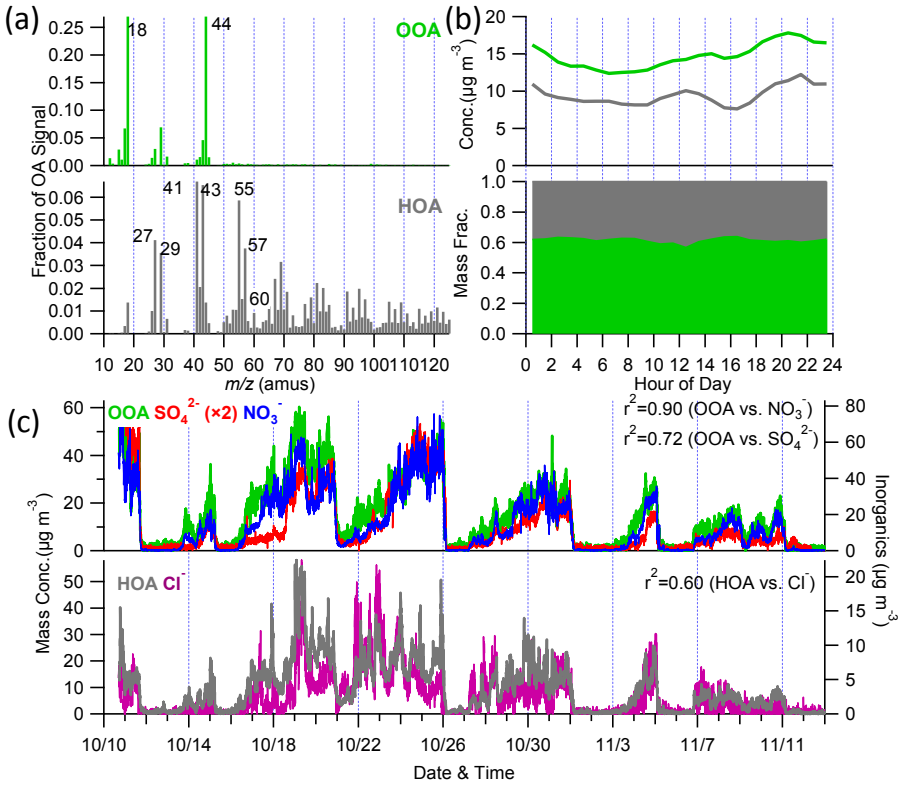

Figure 4. (a) Mass spectra of hydrocarbon-like organic aerosol (HOA) and oxygenated organic aerosol (OOA); (b) diurnal variations of the mass concentration and mass fraction of HOA and OOA; and (c) time series of HOA, OOA, and inorganic species (SO_4^{2-}, NO_3^-, Cl^-). The correlations of HOA and OOA with inorganic species are also shown in the figure.

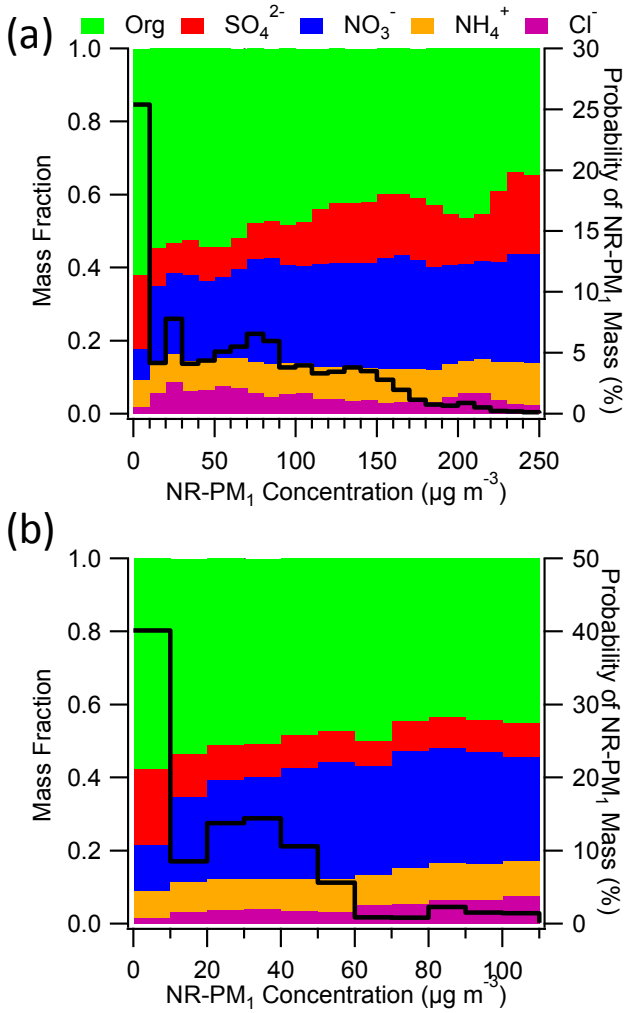

1004

1005 **Figure 5.** Submicron aerosol composition as a function of non-refractory submicron
1006 aerosol ($NR\text{-}PM_1$) mass loadings (a) before the Asia–Pacific Economic Cooperation
1007 (APEC) summit and (b) during APEC. The solid line shows the probability of the
1008 $NR\text{-}PM_1$ mass.

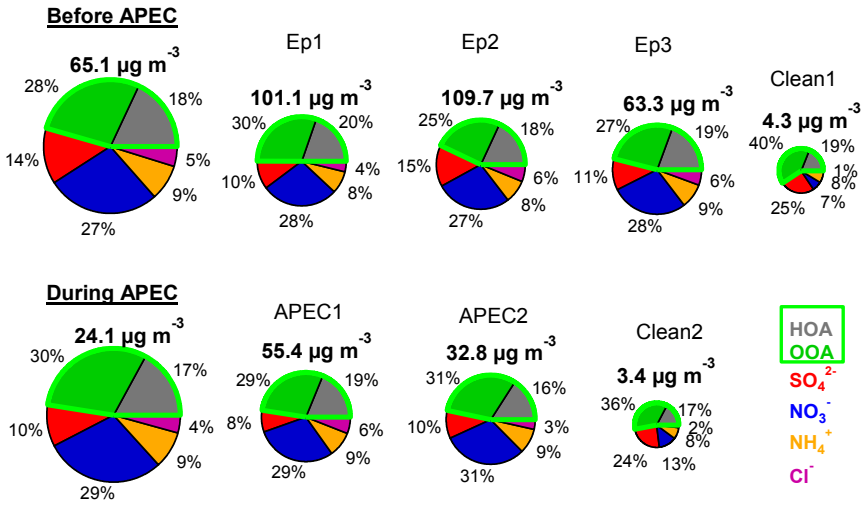

Figure 6. Average chemical composition of non-refractory submicron aerosol ($NR\text{-}PM_1$) before and during the Asia–Pacific Economic Cooperation (APEC) summit and that of five haze episodes and two clean events marked in Fig. 2.

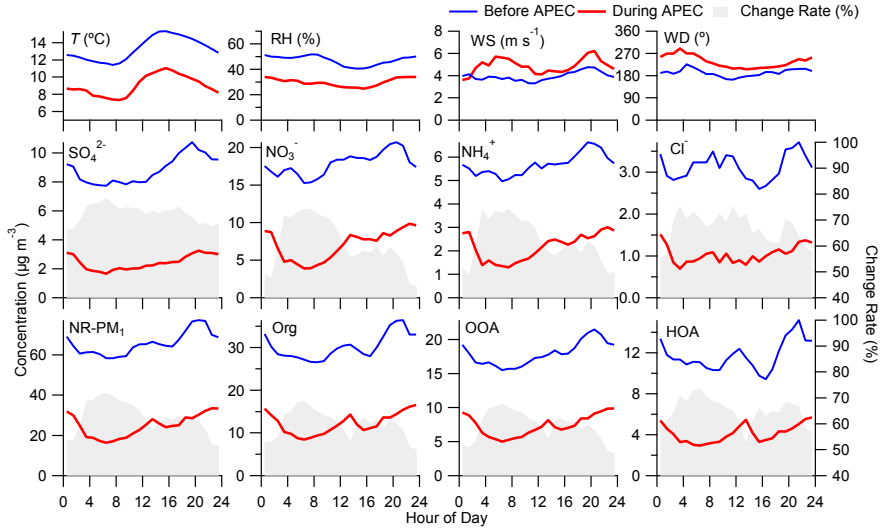

Figure 7. Diurnal variations of meteorological variables such as temperature (*T*), relative humidity (RH), wind speed (WS), and wind direction (WD); non-refractory submicron aerosol ($NR\text{-}PM_1$) species; and organic aerosol (OA) factors before and during the Asia–Pacific Economic Cooperation (APEC) summit. The change rates during APEC (= (Before APEC–APEC)/Before APEC × 100) are also marked in light gray in the figure.

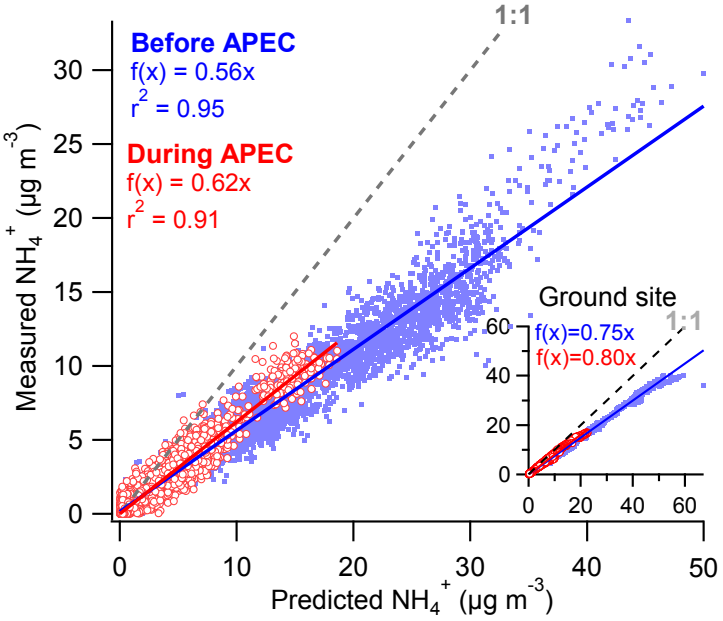

1020

1021 **Figure 8.** Correlations between measured NH_4^+ and predicted NH_4^+ (= 18 × (2 ×
1022 $SO_4^{2-}/96 + NO_3^-/62 + Cl^-/35.5$)) before and during the Asia–Pacific Economic
1023 Cooperation (APEC) summit. The inset plot shows the correlations of measured NH_4^+
1024 versus predicted NH_4^+ at the ground site.

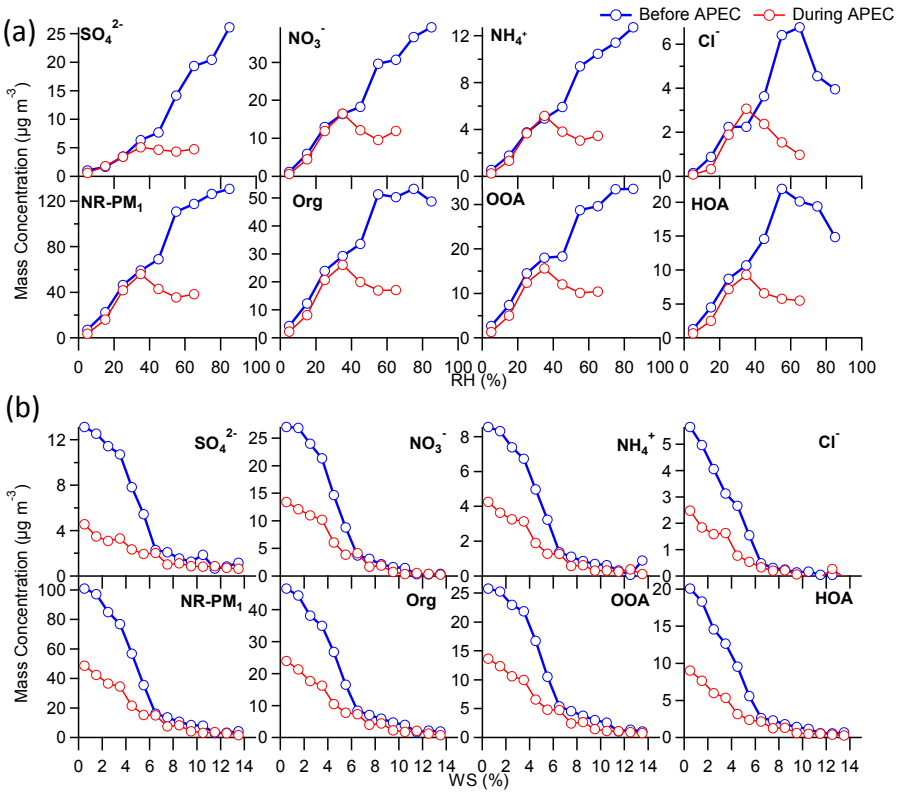

1025

1026 **Figure 9.** Variations of non-refractory submicron aerosol (NR-PM_1) species and
1027 organic aerosol (OA) factors as a function of (a) relative humidity (RH) and (b) wind
1028 speed (WS) before and during the Asia–Pacific Economic Cooperation (APEC)
1029 summit. The RH and WS were from the tower measurements at 280 m.

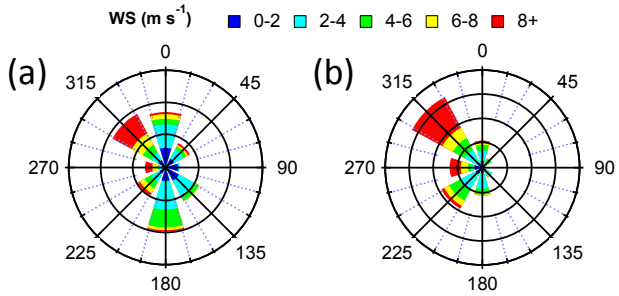

1030

1031 **Figure 10.** Wind increase plots (a) before the Asia–Pacific Economic Cooperation
1032 (APEC) summit and (b) during APEC.

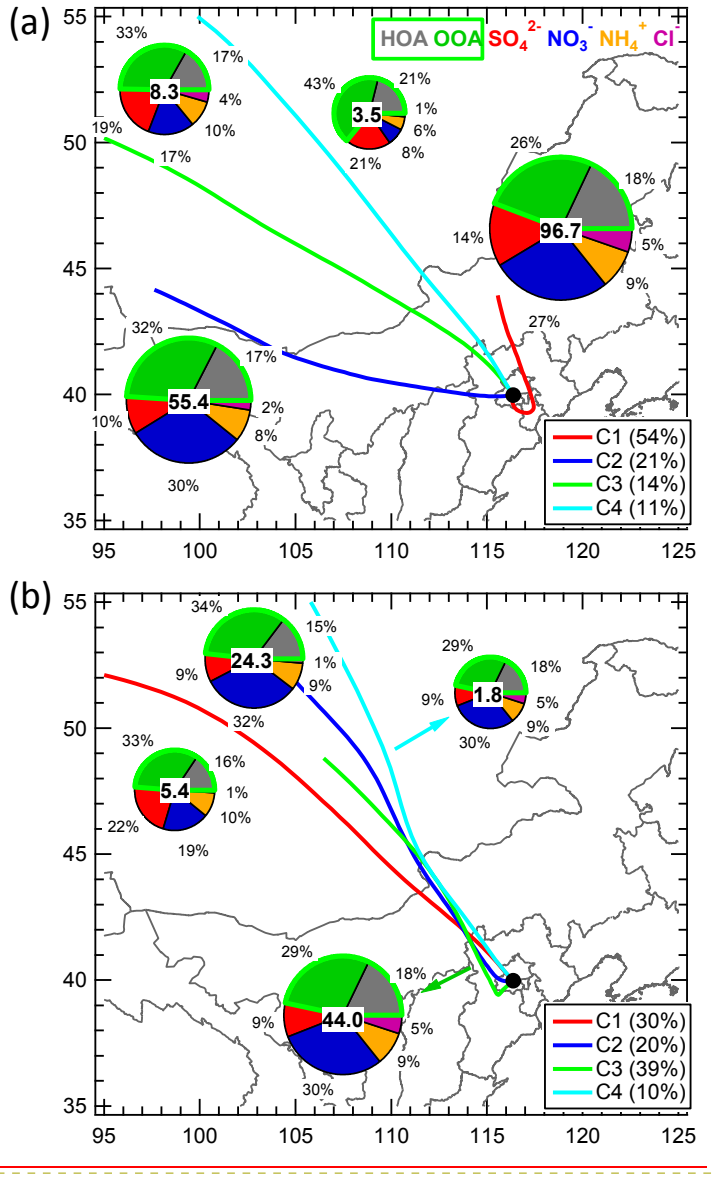

1033

Formatted: Font: (Default) Times New Roman

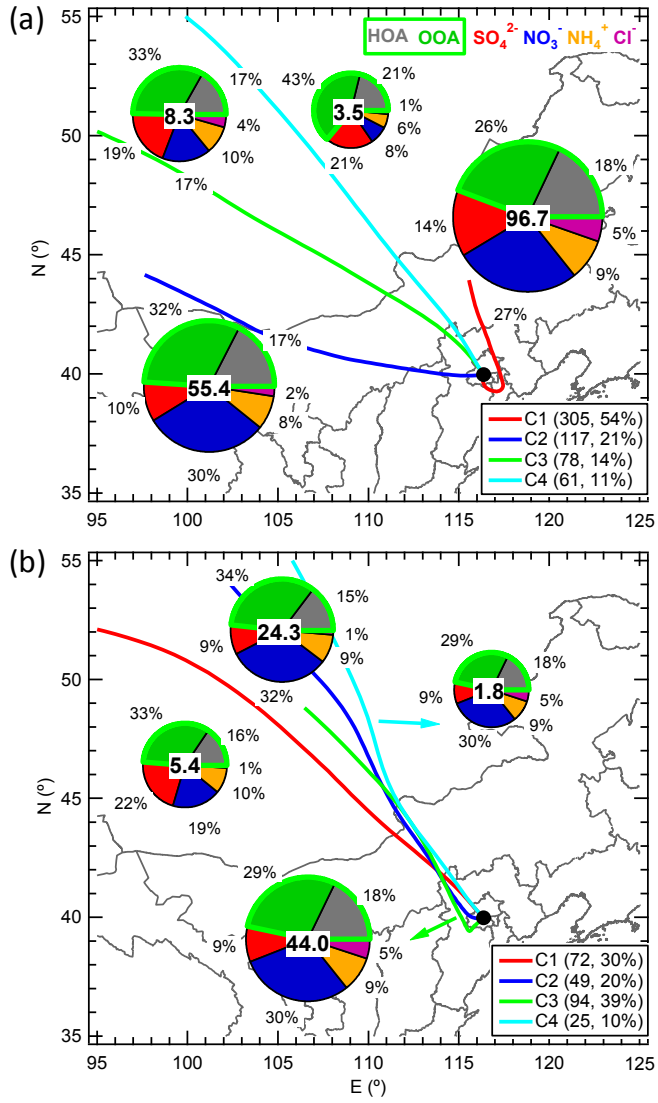

Figure 11. Average non-refractory submicron aerosol (NR-PM_1) composition for each cluster (a) before and (b) during the Asia–Pacific Economic Cooperation (APEC) summit. The numbers on the pie charts refer to the average total NR-PM_1 mass for each cluster. In addition, the number of trajectories and its percentage to the total trajectories are also shown in the legends.

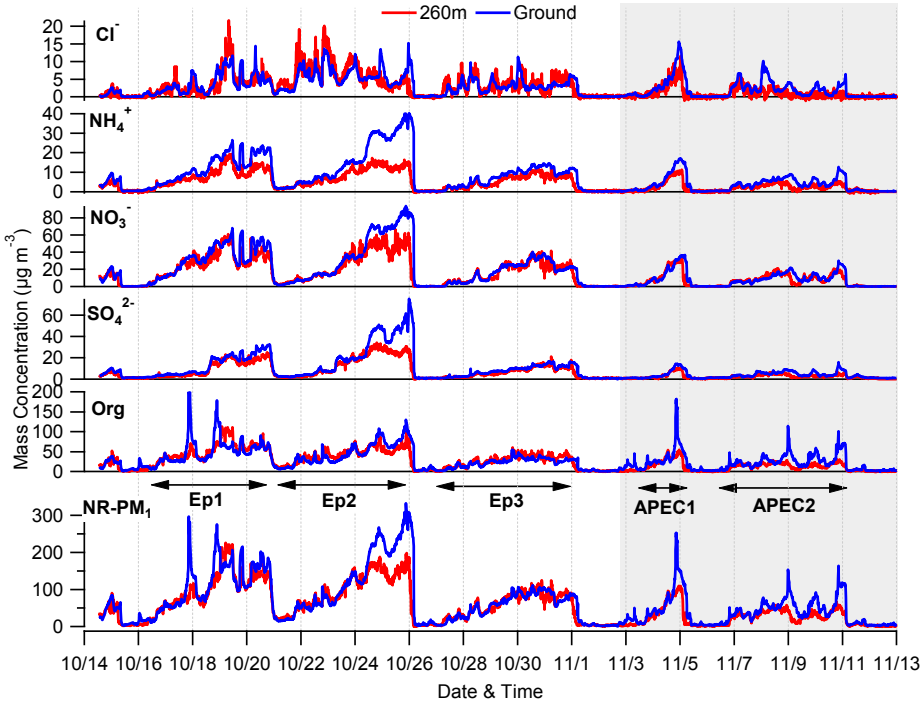

1040

1041 **Figure 12.** Comparisons of time series of total non-refractory submicron aerosol
1042 (NR-PM_1) mass and NR-PM_1 species between 260 m and the ground level.

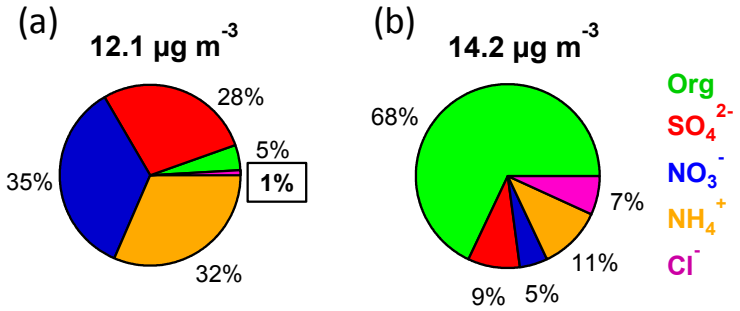

1043

1044 **Figure 13.** Average chemical composition of the difference between ground level and
1045 260 m (a) before the Asia–Pacific Economic Cooperation (APEC) summit and (b)
1046 during APEC. "1%" shown in the box indicates a lower concentration of chloride at
1047 the ground site than that at 260 m.

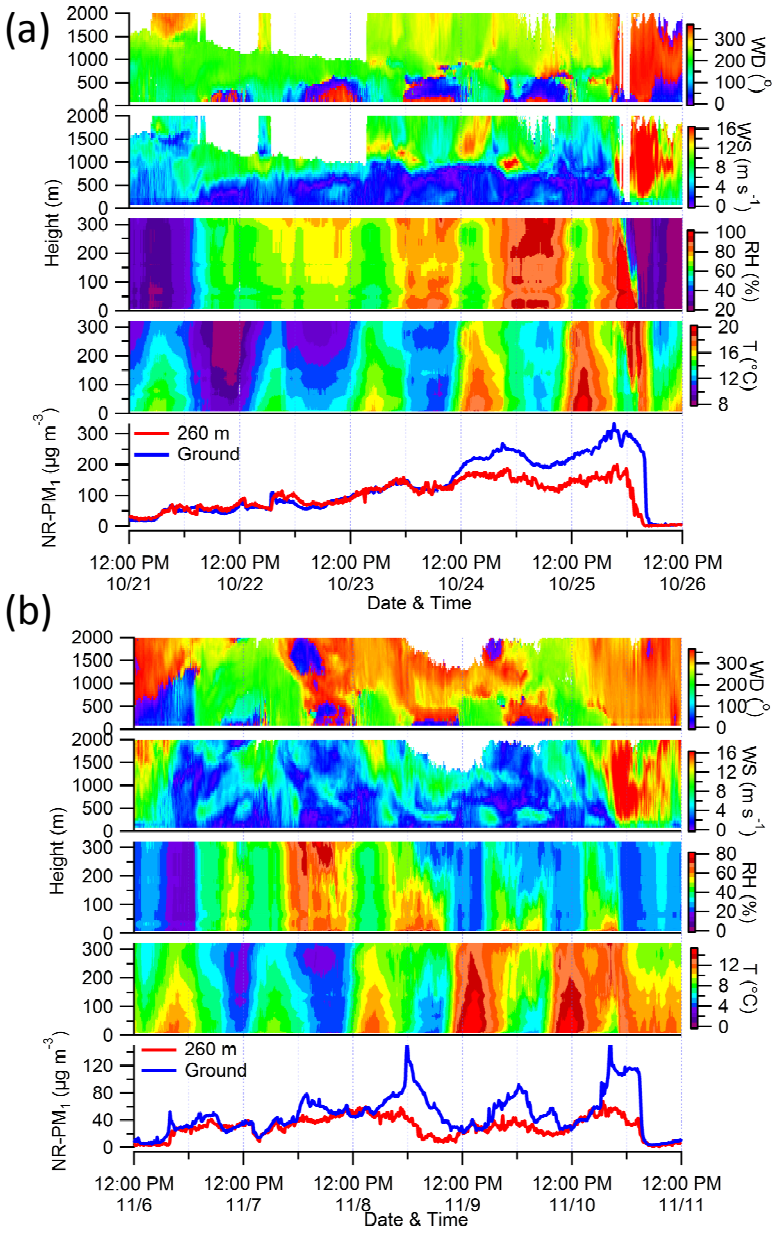

Figure 14. Evolution of vertical profiles of meteorological variables such as wind direction (WD), wind speed (WS), relative humidity (RH), and temperature (*T*) and non-refractory submicron aerosol ($NR\text{-}PM_1$) concentration at 260 m and the ground site during two pollution episodes (a) Ep2 and (b) APEC2. The vertical profiles of wind speed and wind direction were from the measurements of the Doppler wind lidar, and those of RH and T were from the tower measurements. The white areas in the figure indicate that the data were not available.